

Combined Higgs Boson Property Measurements using the ATLAS Detector



Pere Rados
The University of Melbourne, CoEPP
On behalf of the ATLAS Collaboration



Introduction and outline

Since the discovery in 2012 of a new Higgs-like particle with mass ~ 125 GeV, one of the main goals of the ATLAS and CMS experiments has been to measure its properties as precisely as possible.

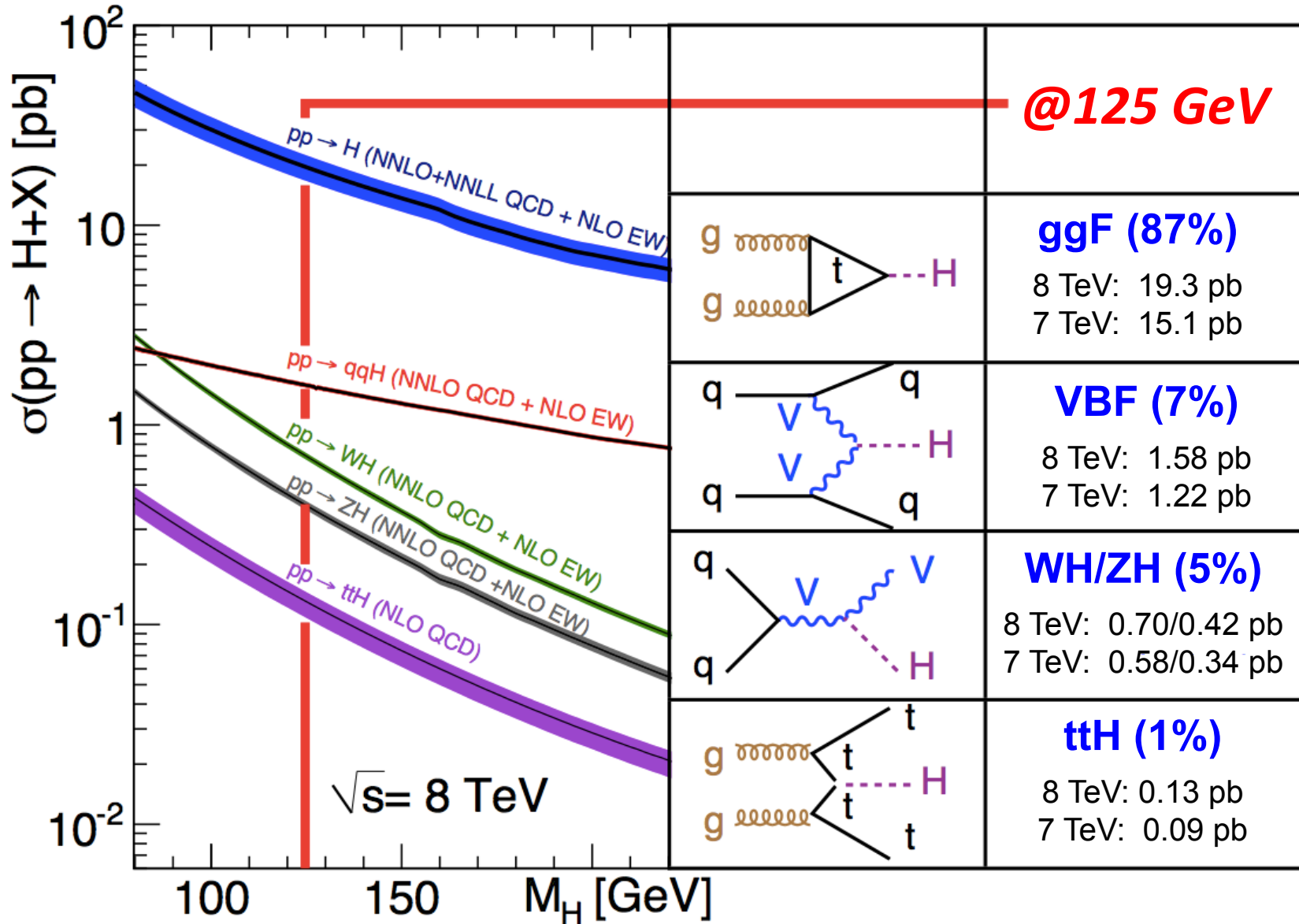


In this talk, the combined measurements of the properties of the Higgs boson using the ATLAS run-1 dataset (25 fb^{-1}) will be summarized.

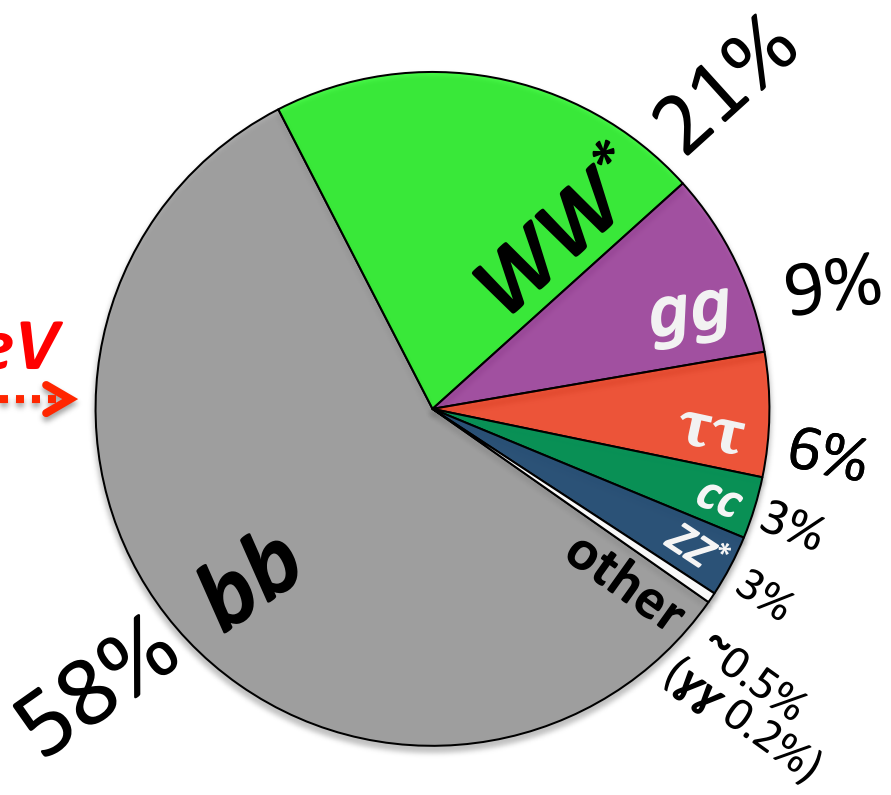
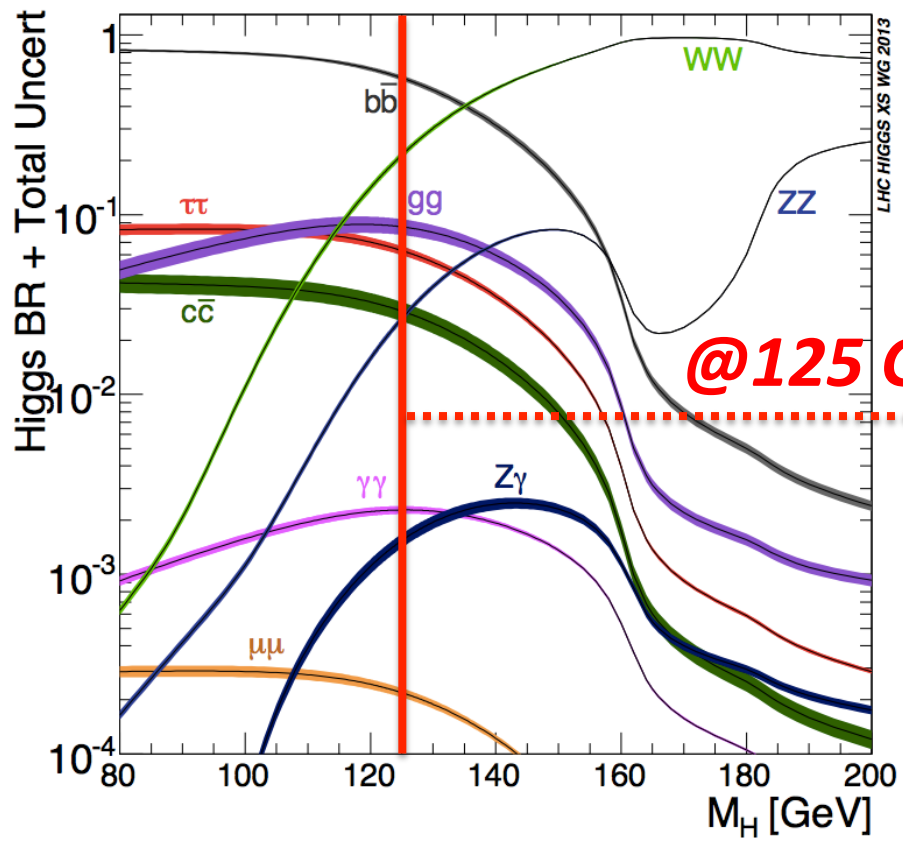
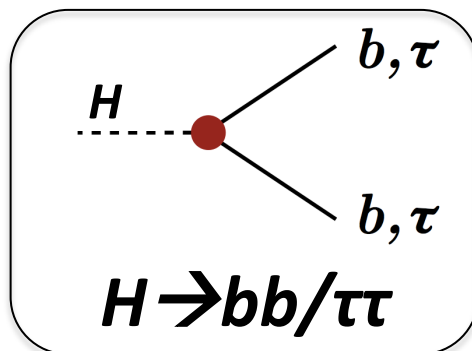
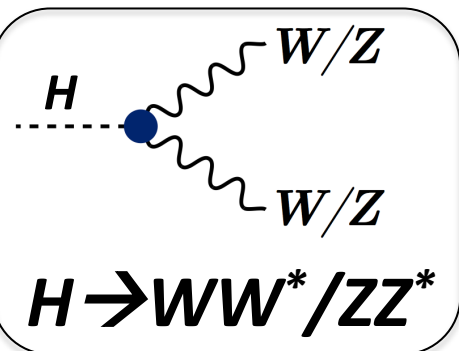
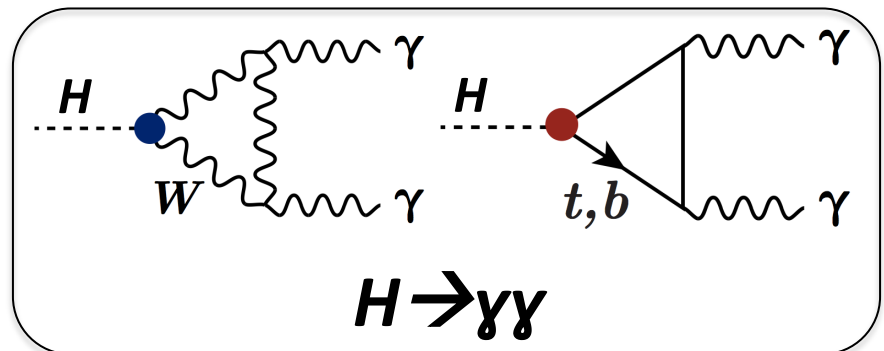
Outline:

- 1) Overview of Higgs production/decay, and the ATLAS detector
- 2) Combined mass
- 3) Combined production/decay rates
- 4) Combined couplings
- 5) Combined spin and parity
- 6) Summary

Higgs production at the LHC

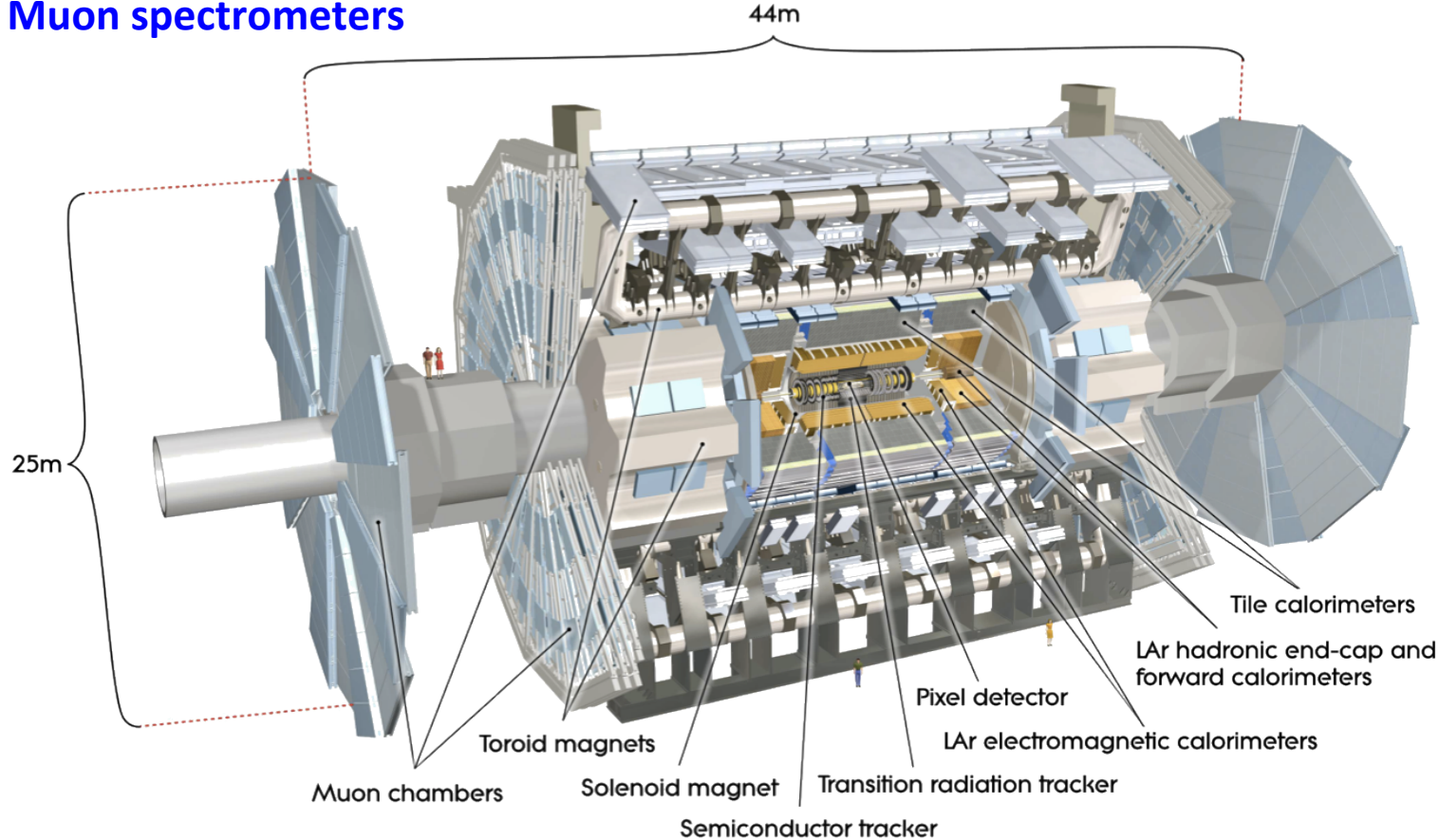


Higgs decay



ATLAS detector

- General purpose detector @LHC comprised of three main sub-detector elements
 - **Trackers:** Pixel detector, SCT and TRT
 - **Calorimeters:** electromagnetic and hadronic (liquid argon, scintillating plates)
 - **Muon spectrometers**

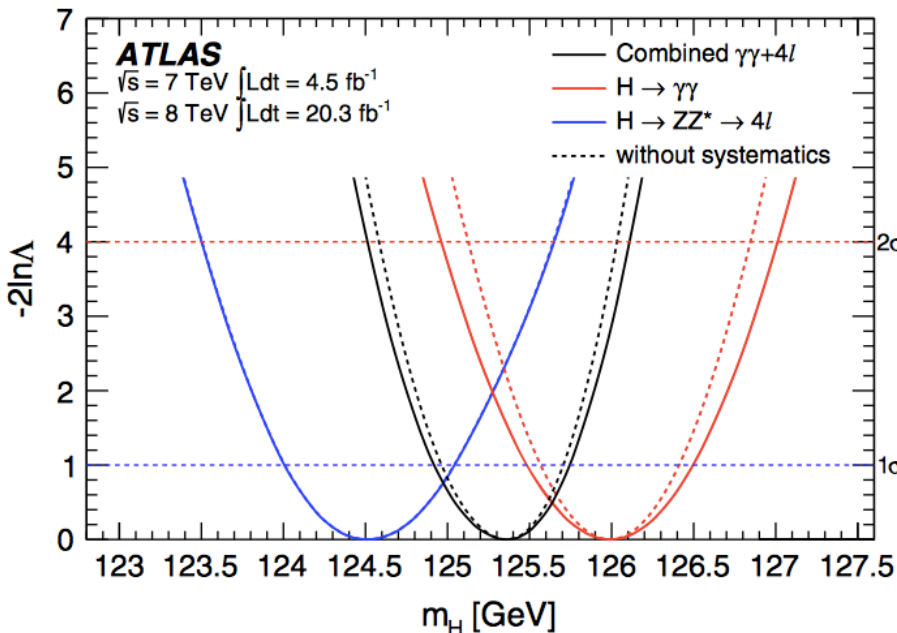


Run-1 integrated luminosity: **20.3 fb⁻¹ @ 8 TeV** **4.7 fb⁻¹ @ 7 TeV**

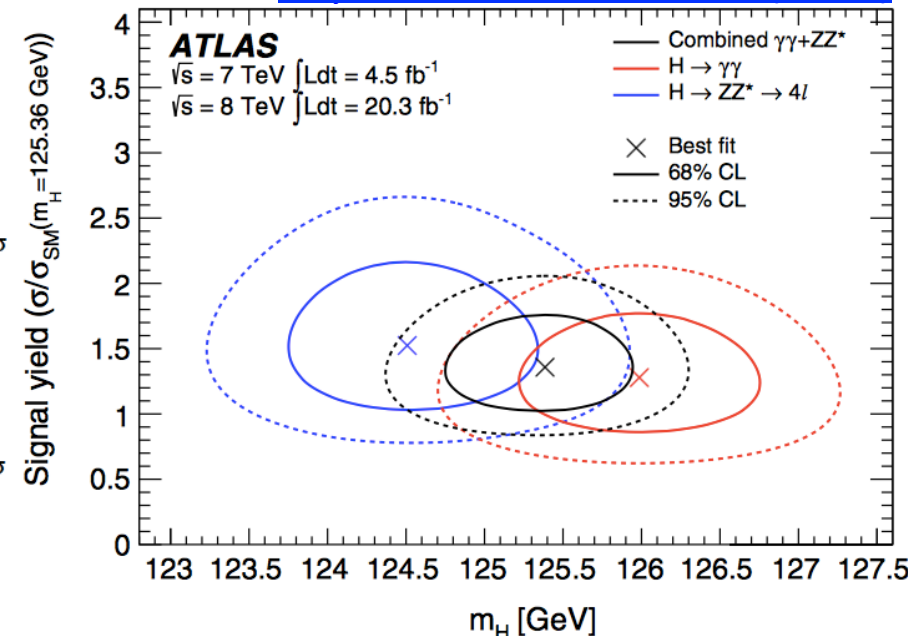
Combined mass

Combined measurements from $H \rightarrow \gamma\gamma$ and $H \rightarrow ZZ^* \rightarrow 4l$ decay channels

- $H \rightarrow \gamma\gamma$: 10 categories based on photon conversion, η , and $p_T^{\gamma\gamma}$ orthogonal to thrust axis
 $m_{\gamma\gamma}$ fit: exponential + crystal ball
- $H \rightarrow ZZ^* \rightarrow 4l$: 4 categories based on lepton flavor (4e, 4 μ , 2e2 μ , 2 μ 2e)
2D fit of m_{4l} and BDT-output



[Phys. Rev. D. 90, 052004 \(2014\)](#)



Channel	Mass measurement [GeV]	$\gamma\gamma-ZZ$ compatibility @ 2.0σ (4.8%)	0.3% precision!
$H \rightarrow \gamma\gamma$	$125.98 \pm 0.42(\text{stat}) \pm 0.28(\text{syst}) = 125.98 \pm 0.50$		
$H \rightarrow ZZ^* \rightarrow 4\ell$	$124.51 \pm 0.52(\text{stat}) \pm 0.06(\text{syst}) = 124.51 \pm 0.52$		
Combined	$125.36 \pm 0.37(\text{stat}) \pm 0.18(\text{syst}) = 125.36 \pm 0.41$		

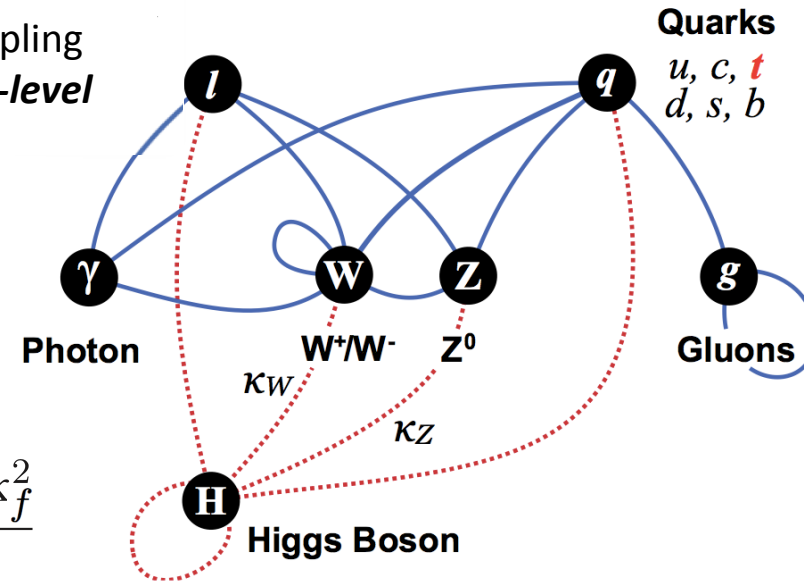
Production/decay rates and couplings

- Combination includes results from $H \rightarrow \gamma\gamma$, ZZ^* , WW^* , $\tau\tau$, $b\bar{b}$, $\mu\mu$, $Z\gamma$ analyses, and constraints on $t\bar{t}H$ and off-shell Higgs production. [arXiv:1507.04548 \(2015\)](https://arxiv.org/abs/1507.04548)

- κ -framework:** search for deviations of SM Higgs coupling to other particles by introducing multipliers using *tree-level motivated benchmark model* following the LHC Higgs WG recommendations ([arXiv:1307.1347](https://arxiv.org/abs/1307.1347))

- Assumptions:
 - Single, narrow, CP-even scalar resonance (tensor structure of couplings assumed to be those of SM)
 - Narrow width approximation is valid:

$$\sigma \mathcal{B}(i \rightarrow H \rightarrow f) = \frac{\sigma_i \Gamma_f}{\Gamma_H} = \frac{\sigma_i^{SM} \Gamma_f^{SM}}{\Gamma_H^{SM}} \cdot \frac{\kappa_i^2 \cdot \kappa_f^2}{\kappa_H^2}$$



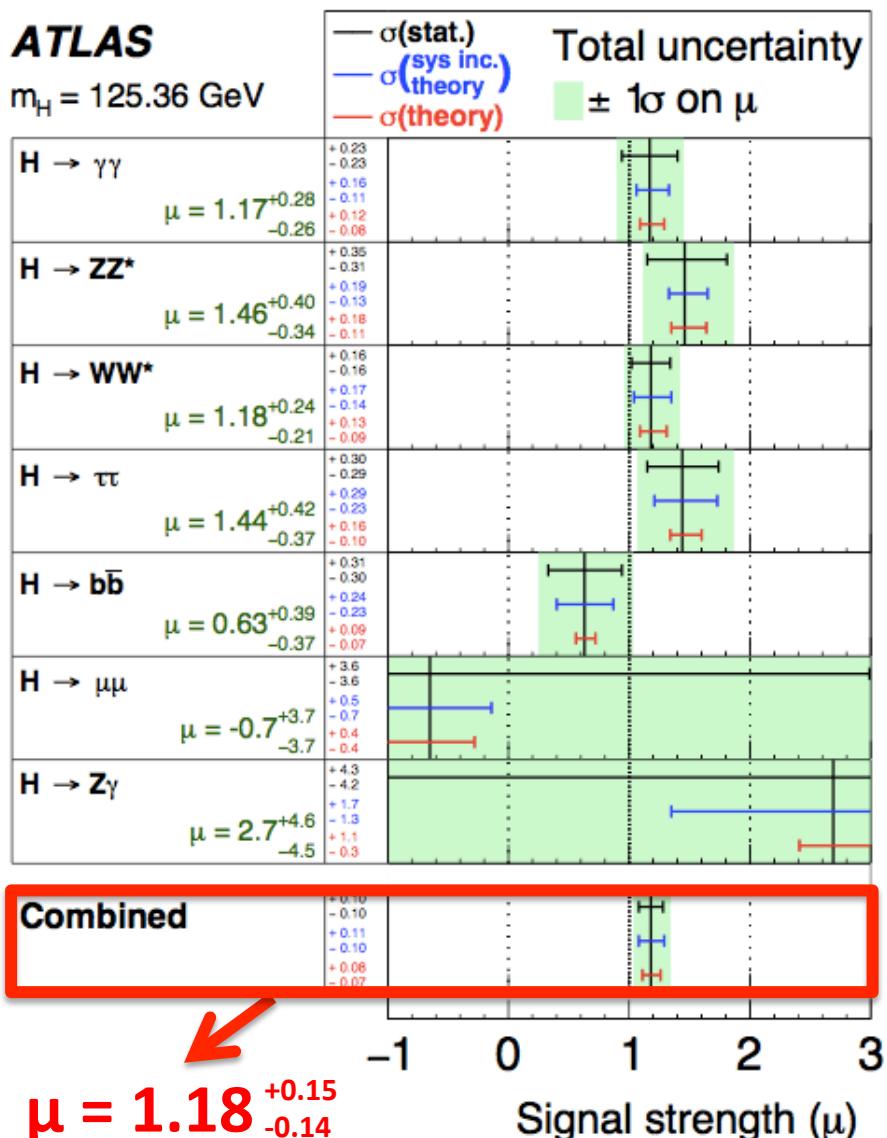
Parameters of interest:

- **Signal strength $\mu = \sigma \times BR / (\sigma \times BR)_{SM}$**
 - the multiplier for total yield (can be defined for each production mode and decay channel)
- **Multipliers κ for a given coupling**
 - Different models tested by imposing different relations between multipliers
 - κ allows more direct access to coupling than μ (complex interplay between prod./decay)
- **In both cases, SM has $\mu = 1.0$ and $\kappa = 1.0$**

Combined signal strengths

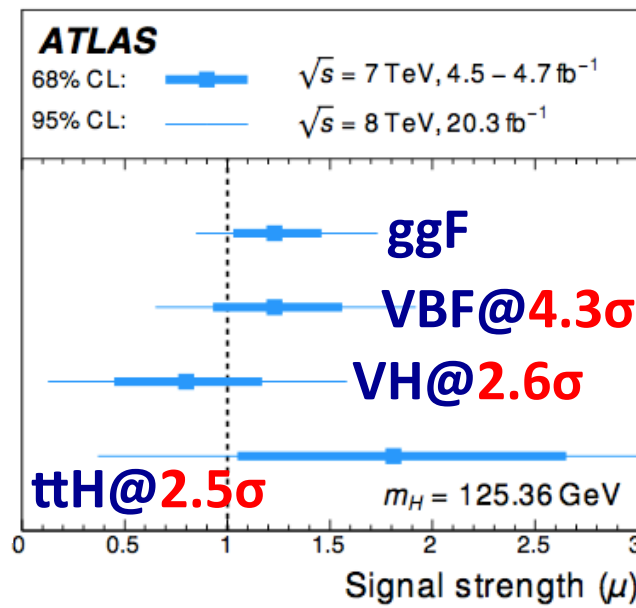
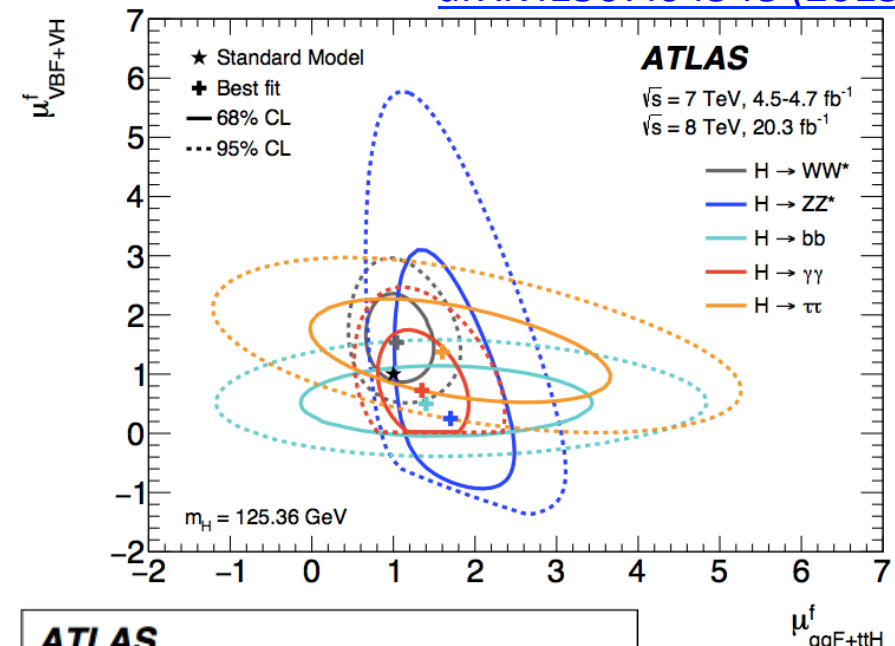
ATLAS

$m_H = 125.36 \text{ GeV}$



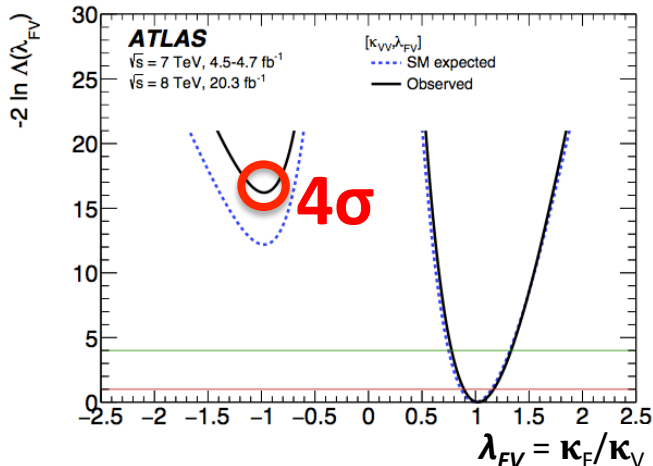
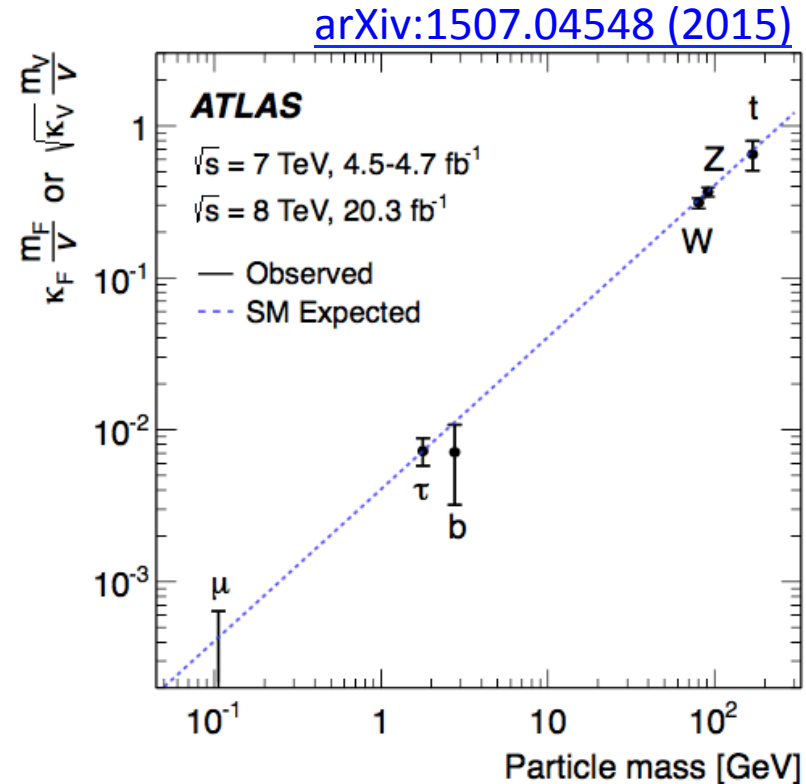
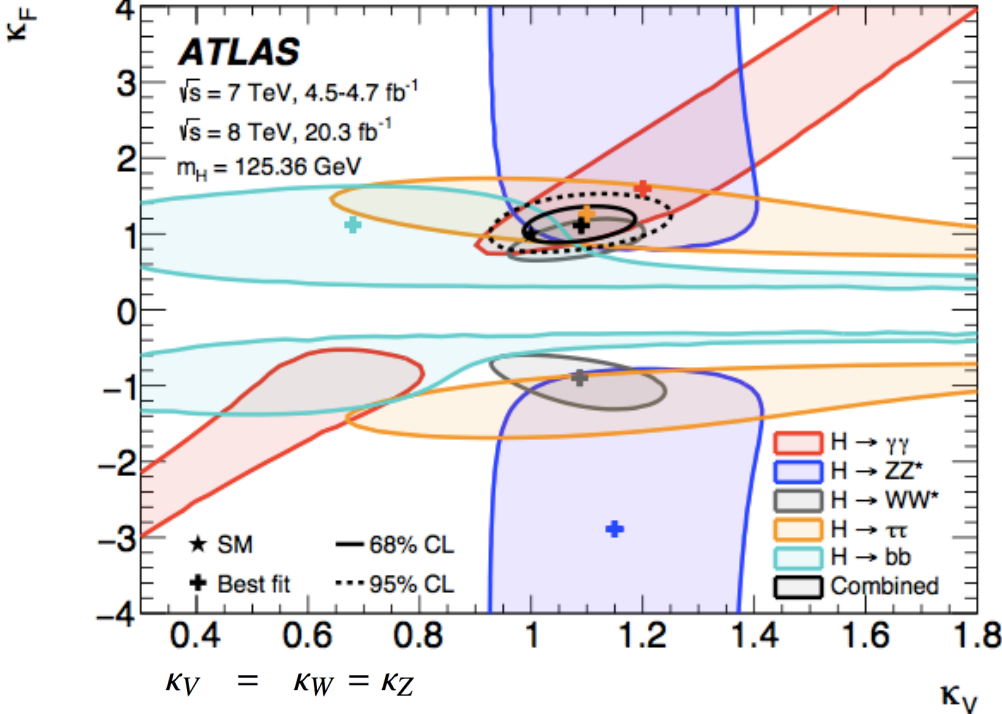
(18% SM compatibility)

arXiv:1507.04548 (2015)



Signal strength by production mode assumes the SM values of Higgs BRs

Combined couplings



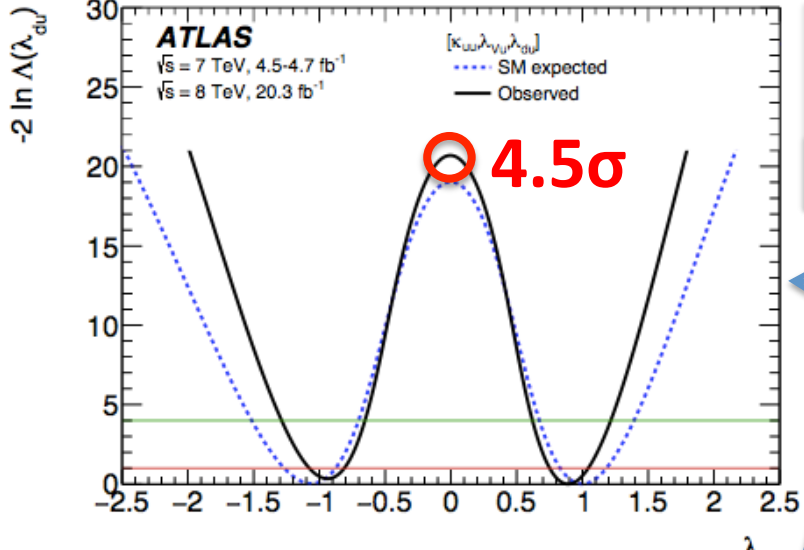
Best fit value when other parameter is profiled:
 $\kappa_V = 1.09^{+0.07}_{-0.07}$ $\kappa_F = 1.11^{+0.17}_{-0.15}$ (41% SM compatibility)

Here, the κ_V - κ_F fit assumes only SM contributions to Γ_H

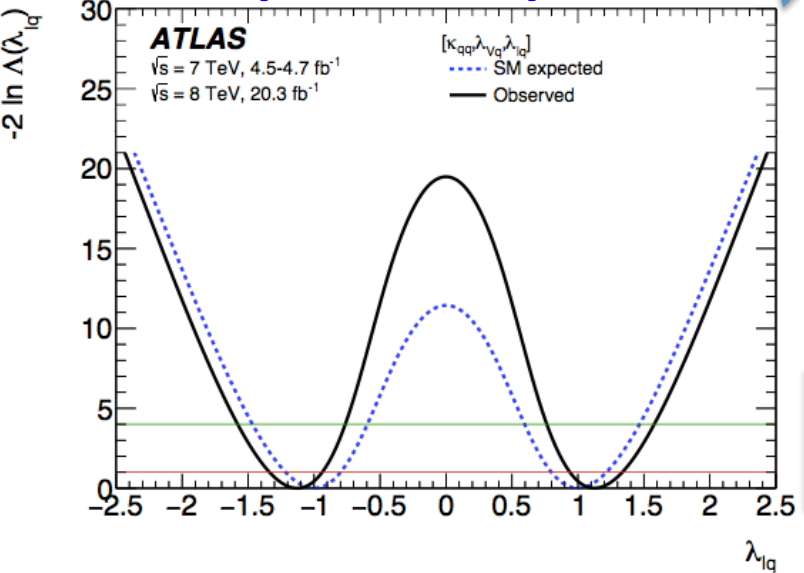
Best fit value on the ratio:
 $\lambda_{FV} = 1.02^{+0.15}_{-0.13}$ (negative κ_F disfavored at ~4 σ level)

Combined couplings

up- vs down-type



quark vs lepton



Best fit value for κ_d / κ_u :

$$\lambda_{du} \in [-1.08, -0.81] \cup [0.75, 1.04] \quad (68\% \text{ CL})$$

Coupling to down-type fermions @ $\sim 4.5\sigma$

sensitive to SUSY

sensitive to additional particles in loops

sensitive to unobserved/invisible particles

ATLAS

68% CL: — $\sqrt{s} = 7 \text{ TeV}, 4.5\text{--}4.7 \text{ fb}^{-1}$
95% CL: — $\sqrt{s} = 8 \text{ TeV}, 20.3 \text{ fb}^{-1}$

Here, assumes that couplings of other SM particles are as predicted by SM.

$$K_Y = 1.00 \pm 0.12$$

$$K_g = 1.12^{+0.14}_{-0.11}$$

$$(95\% CL) \quad \kappa_{ZY} < 3.3$$

$$(95\% CL) \quad BR_{i,u.} < 0.27$$

$$\frac{\Gamma_H}{\Gamma_H^{\text{SM}}} = 1.03^{+0.13}_{-0.03}$$

$$m_H = 125.36 \text{ GeV}$$

Parameter value

Best fit value for κ_l / κ_q :

$$\lambda_{lq} \in [-1.34, -0.94] \cup [0.94, 1.34] \quad (68\% \text{ CL})$$

Spin and parity

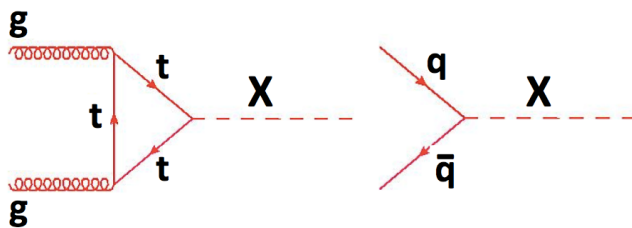
Options for spin and parity of the Higgs

- New boson decays to pair gauge bosons with total charge 0
 - integer **spin**: **0, 1 or 2**
- Observation of $H \rightarrow \gamma\gamma$
 - **spin 1** strongly disfavored (Landau-Yang theorem), and ruled out at >99% CL in previous ATLAS publications
- **Parity** of the new boson to be determined

Recall that the SM Higgs boson is spin-0 and CP-even
 $J^P = 0^+$

Exclude alternative hypothesis in favor of SM (**0⁺**):

- **0⁻**: ggF production
- **0⁺_h**: ggF production
- Mixture of **0⁺** and **0⁻ / 0⁺_h**
- **2⁺** (graviton-like tensor): ggF and qbarq production



Models rely on EFT, only H @ 125.4 GeV considered:

- Valid up to **$\Lambda \sim 1$ TeV** as minimum mass for BSM particles

$$\mathcal{L}_0^V = \left\{ \cos(\alpha) \kappa_{SM} \left[\frac{1}{2} g_{HZZ} Z_\mu Z^\mu + g_{HWW} W_\mu^+ W^{-\mu} \right] - \frac{1}{4} \frac{1}{\Lambda} \left[\cos(\alpha) \kappa_{HZZ} Z_{\mu\nu} Z^{\mu\nu} + \sin(\alpha) \kappa_{AZZ} Z_{\mu\nu} \tilde{Z}^{\mu\nu} \right] - \frac{1}{2} \frac{1}{\Lambda} \left[\cos(\alpha) \kappa_{HWW} W_{\mu\nu}^+ W^{-\mu\nu} + \sin(\alpha) \kappa_{AWW} W_{\mu\nu}^+ \tilde{W}^{-\mu\nu} \right] \right\} X_0.$$

CP-even **CP-odd** $\tilde{\kappa}_{HVV} \sim \kappa_{HVV}$

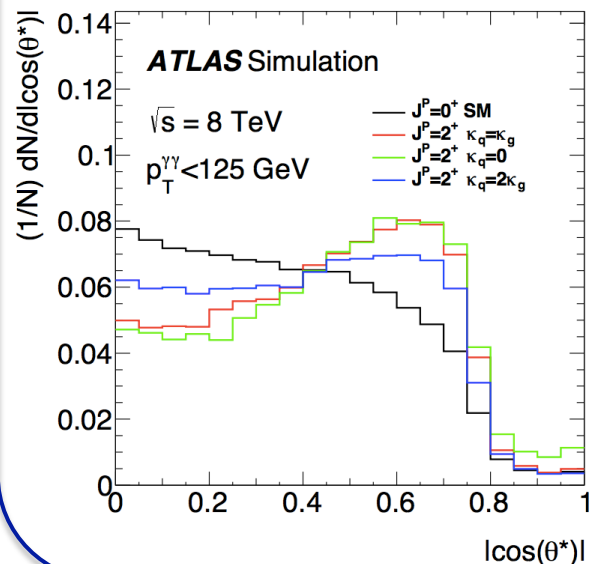
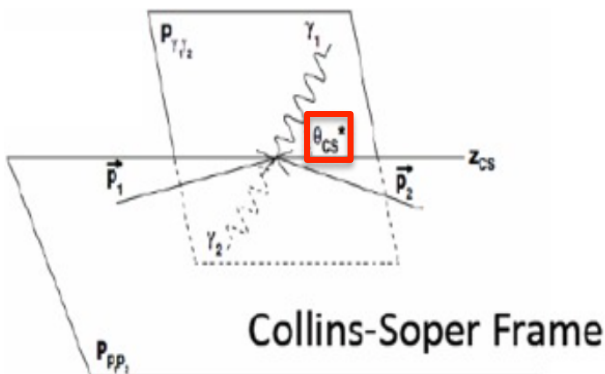
J^P	Model	Values of tensor couplings			
		κ_{SM}	κ_{HVV}	κ_{AVV}	α
0^+	SM Higgs boson	1	0	0	0
0^+_h	BSM spin-0 CP-even	0	1	0	0
0^-	BSM spin-0 CP-odd	0	0	1	$\pi/2$

Spin and parity

H $\rightarrow\gamma\gamma$

Spin-sensitive variables:

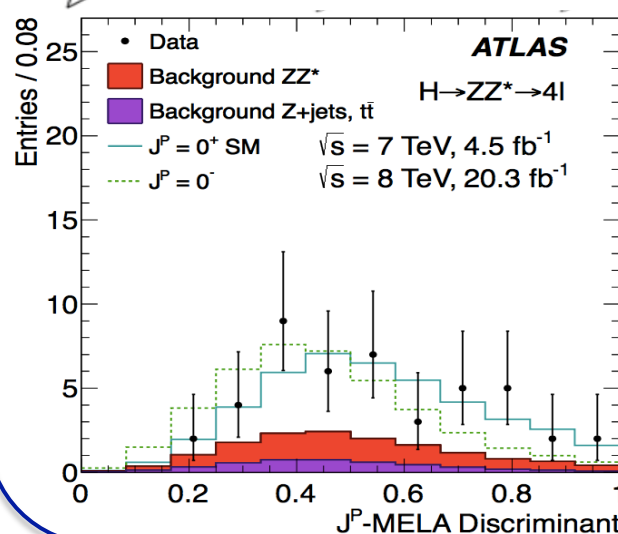
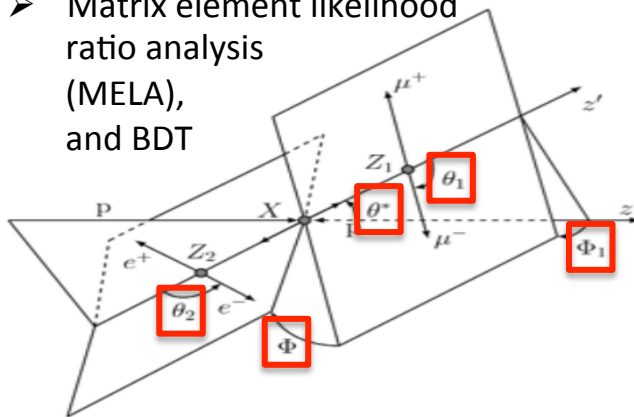
- $p_T^{\gamma\gamma}$, and production of $\gamma\gamma$ in Collins-Soper frame
- 11 categories, fit on final yields



H $\rightarrow ZZ^*\rightarrow 4l$

Spin/parity-sensitive variables:

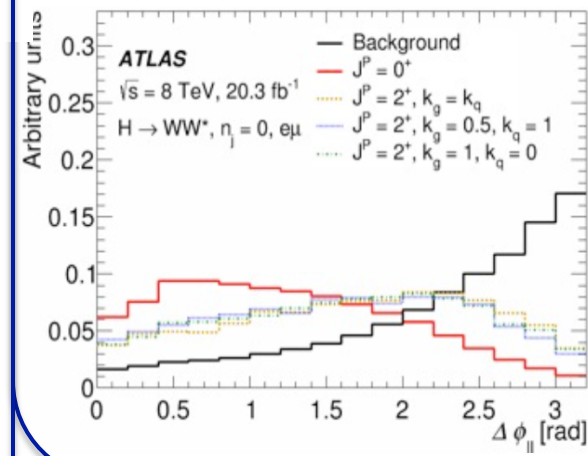
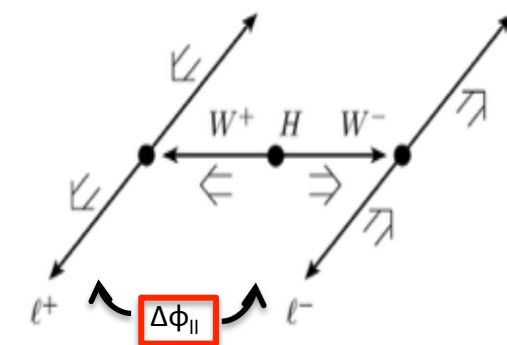
- angular variables of leptons & planes
- Optimal Observables based on ME (go into fit for CP-mixing analysis)
- 4 categories based on lepton flavor
- Matrix element likelihood ratio analysis (MELA), and BDT



H $\rightarrow WW^*\rightarrow e\nu\mu\nu$

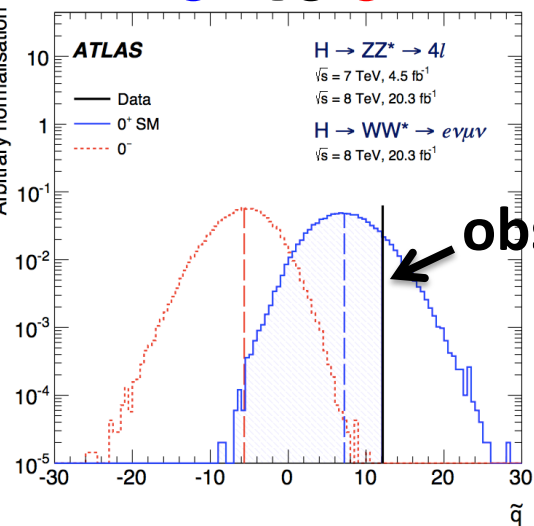
Spin-sensitive variables:

- Four variables: $m_{||}, p_{||}^T, \Delta\phi_{||}$ and m_T
- 1 BDT for SM 0^+ , and 5 BDTS for different spin-2 models

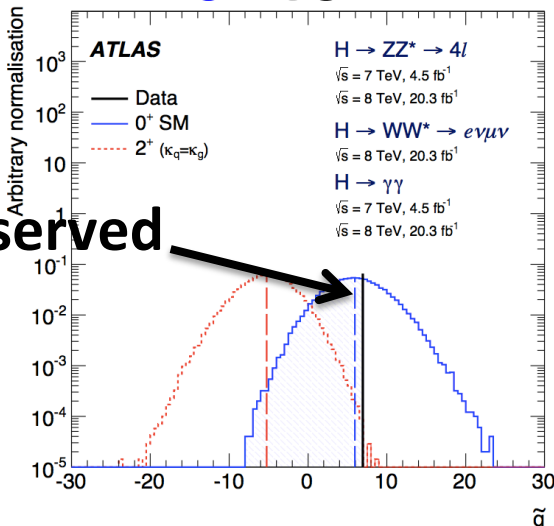


Combined Spin/CP

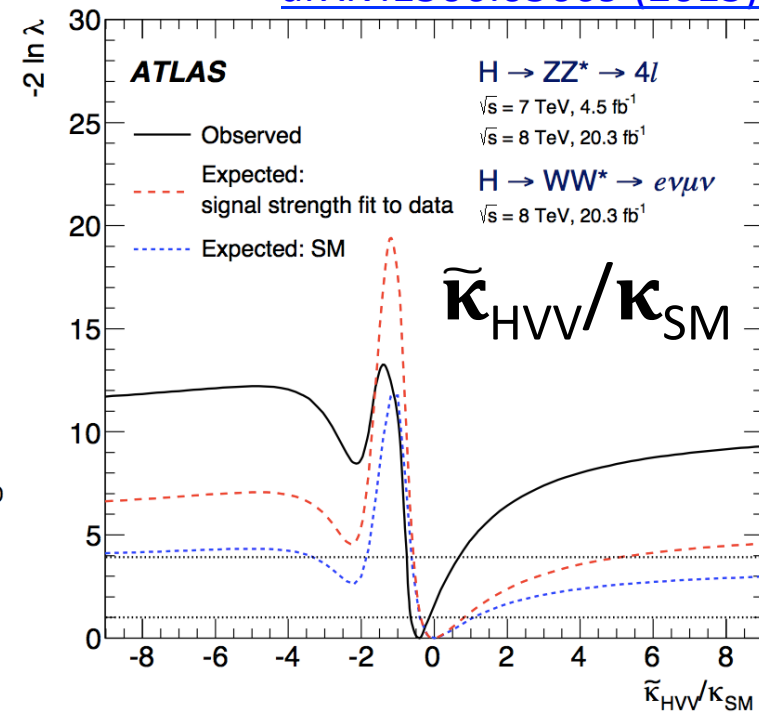
0⁺ vs 0⁻



0⁺ vs 2⁺



Construct test statistic \tilde{q} , to test particular J^P hypothesis against SM Spin/CP assignment (0^+)



Coupling ratio	Best-fit value	95% CL Exclusion Regions	
Combined	Observed	Expected	Observed
$\tilde{\kappa}_{HVV}/\kappa_{SM}$	-0.48	$(-\infty, -0.55] \cup [4.80, \infty)$	$(-\infty, -0.73] \cup [0.63, \infty)$
$(\tilde{\kappa}_{AVV}/\kappa_{SM}) \cdot \tan \alpha$	-0.68	$(-\infty, -2.33] \cup [2.30, \infty)$	$(-\infty, -2.18] \cup [0.83, \infty)$

All alternative spin/CP models excluded at above 99% CL,
in favor of 0⁺ hypothesis (even assuming non-SM couplings to q and g)

Summary

Highlights of the ATLAS run-1 combined Higgs property measurements:

- ❖ Combined mass: **125.36 ± 0.41 GeV**
- ❖ Combined signal strength: **$1.18^{+0.15}_{-0.14}$**
- ❖ Evidence for VBF, VH and ttH production @ **4.3σ , 2.6σ** and **2.5σ**
- ❖ Long list of coupling scenarios have been tested, and **no significant deviations from the SM have been observed**
 - SM compatibilities range from 29-99% for all considered benchmark models
- ❖ Evidence for coupling to down-type fermions @ **4.5σ**
- ❖ All **alternative spin/CP models excluded at >99% CL**, in favor of the SM ($J^P = 0^+$) hypothesis

The **run-1** data has been fully exploited, and ATLAS is now ready to investigate the Higgs boson properties in **run-2** with higher energy collisions and a larger dataset.

So stay tuned!

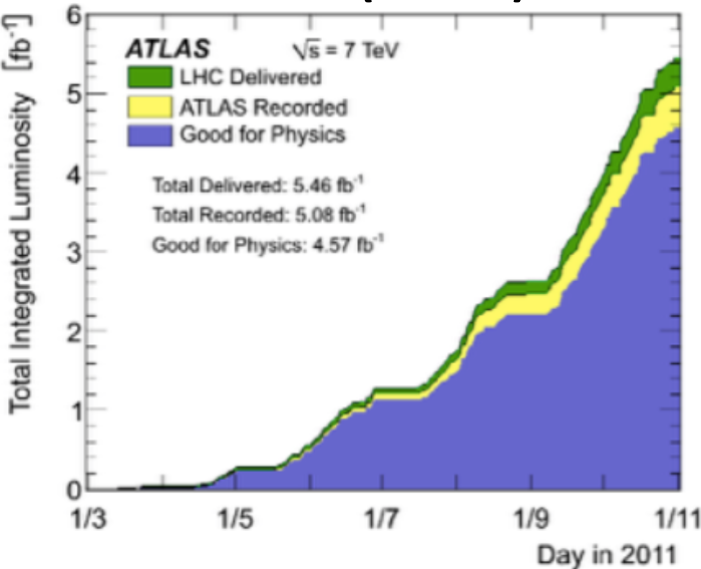
BACKUP

Related Talks

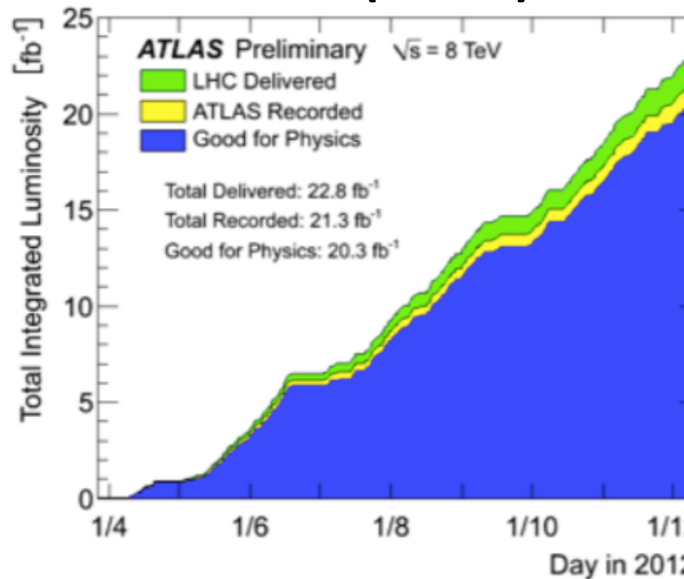
- Tuesday:
 - Overview of SM Higgs Physics from ATLAS and CMS, by Attilio Andreazza
 - Constraints on new phenomena through Higgs coupling measurements with the ATLAS detector, by Lydia Brenner
 - Latest results on the Higgs boson in the diphoton decay channel, by Florian Bernlochner
- Wednesday:
 - Status of Higgs coupling strength determination from ATLAS and CMS, by Maria Llacer
 - Search for the Higgs boson in the ttH production channel using the ATLAS detector, by Julian Bouffard

Run-1 dataset and conditions

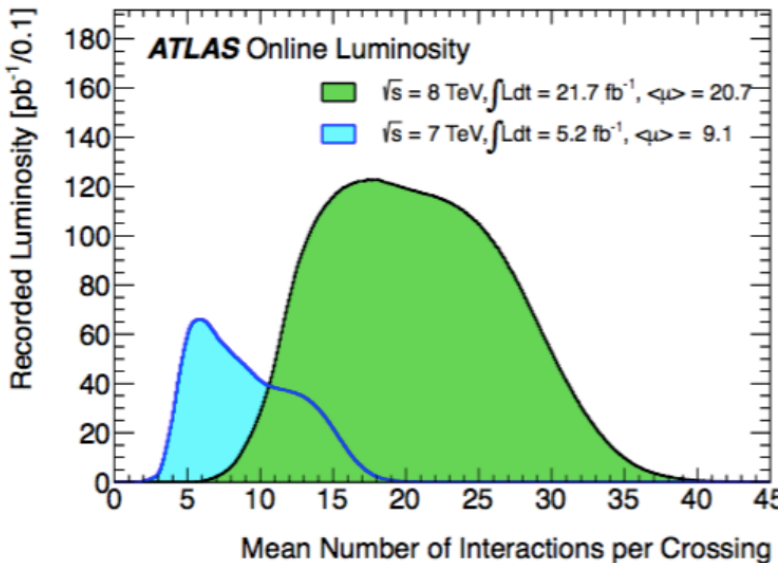
2011 (7 TeV)



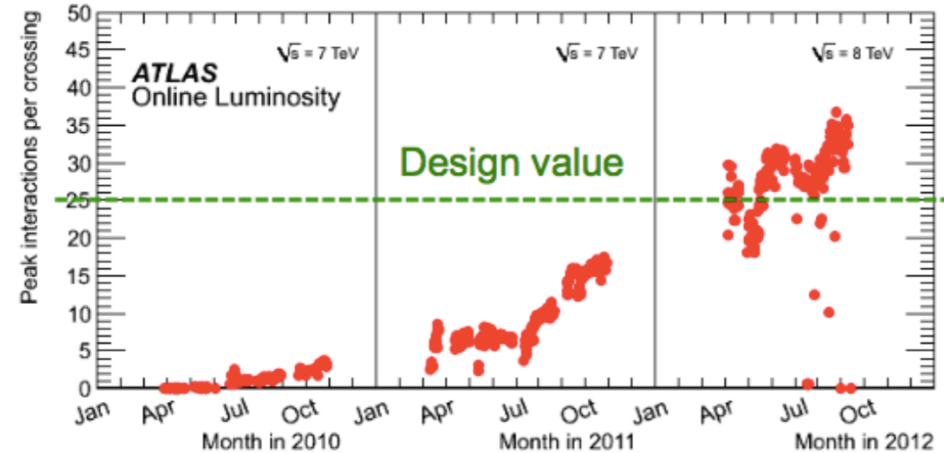
2012 (8 TeV)



95% (90%) of recorded (delivered) luminosity was good for physics analysis.



Challenges with high-luminosity (pile-up)



Higgs production @ LHC (1)

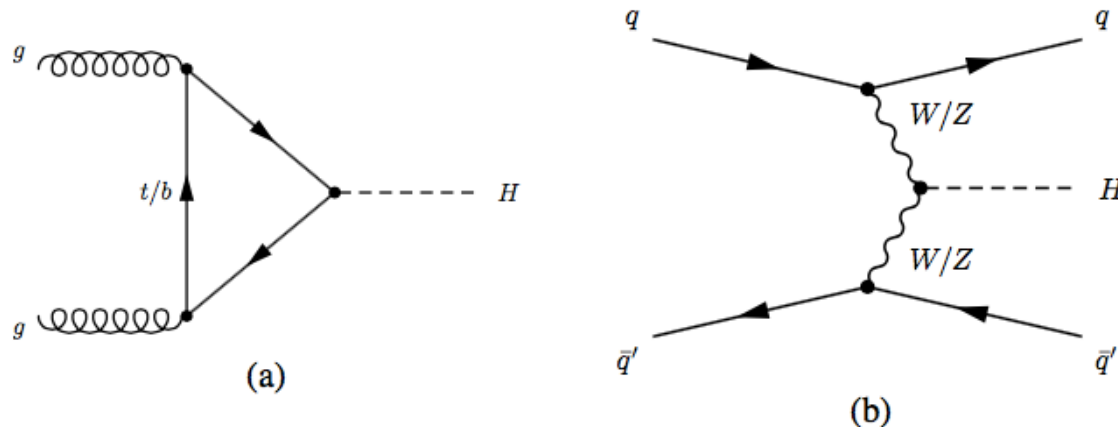


Figure 7: Feynman diagrams of Higgs boson production via (a) the ggF and (b) VBF production processes.

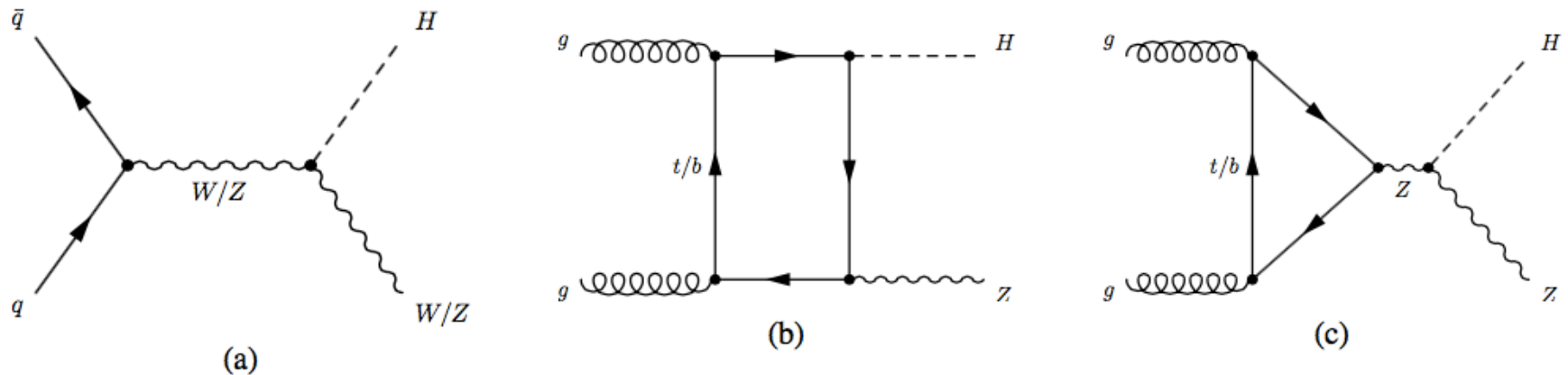


Figure 8: Feynman diagrams of Higgs boson production via (a) the $q\bar{q} \rightarrow VH$ and (b,c) $gg \rightarrow ZH$ production processes.

Higgs production @ LHC (2)

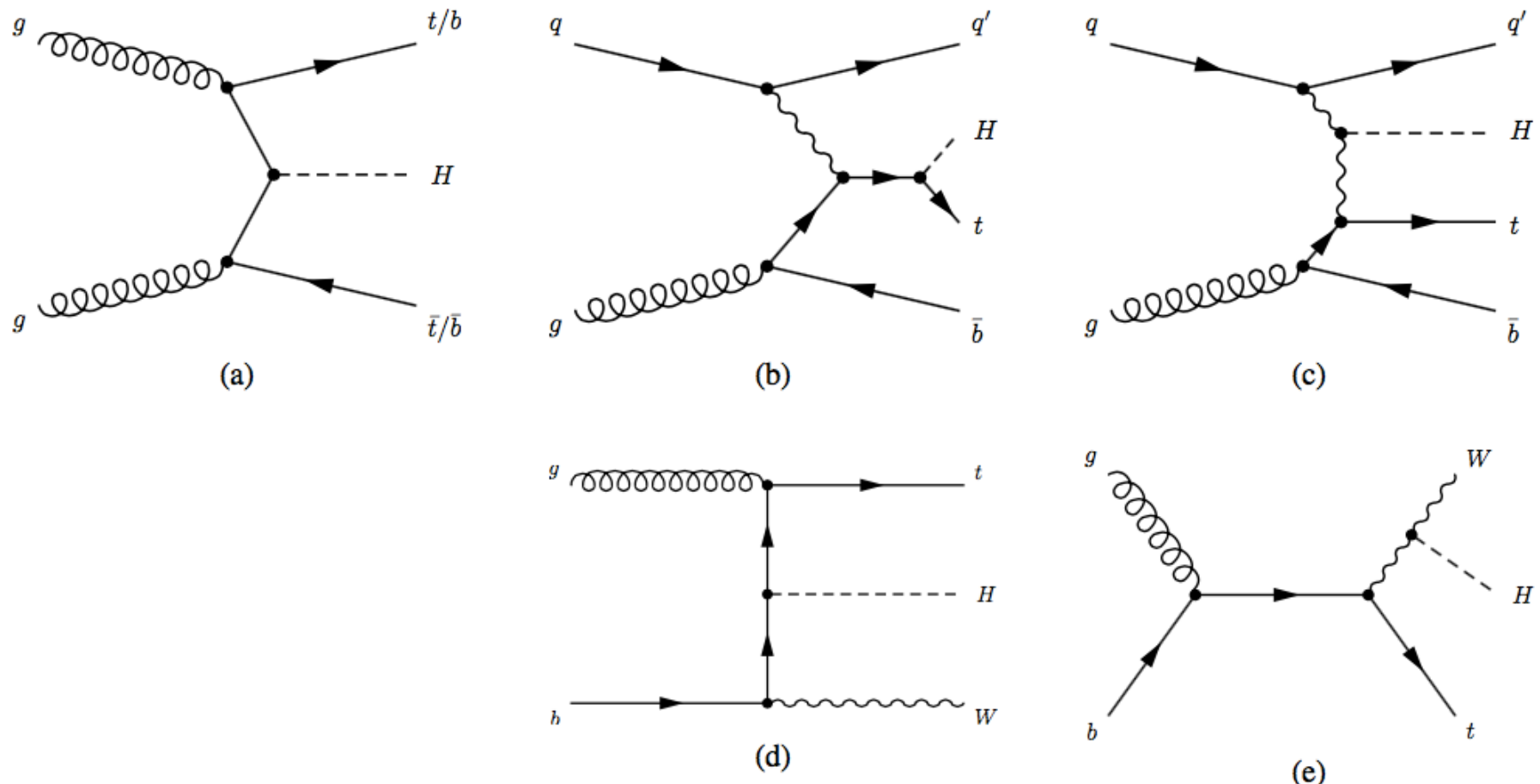
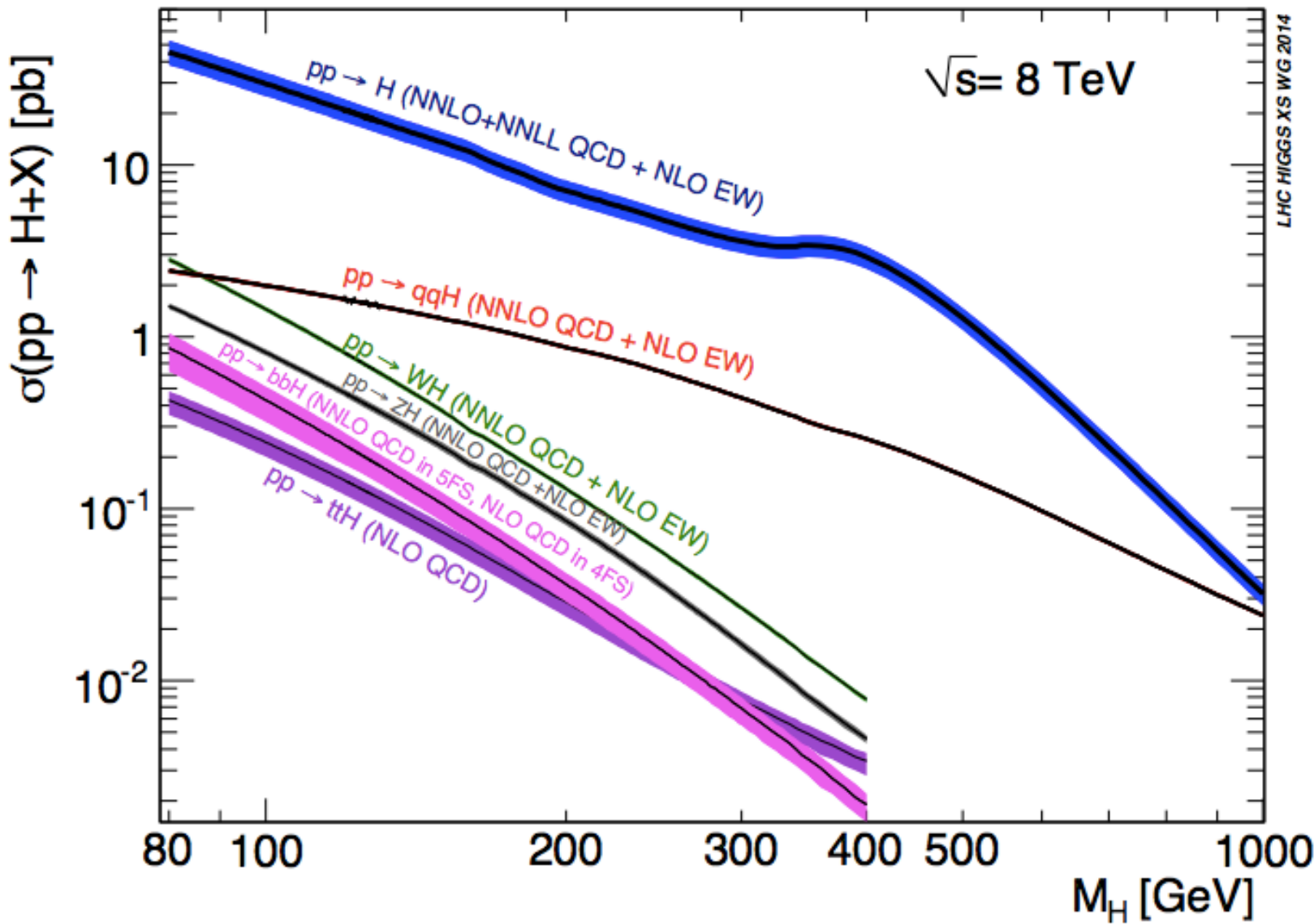


Figure 9: Feynman diagrams of Higgs boson production via (a) the $t\bar{t}H$ (bbH) and (b,c) $tHq'\bar{b}$ (d,e) and WtH processes.

Higgs production @ LHC (3)



Signal MC

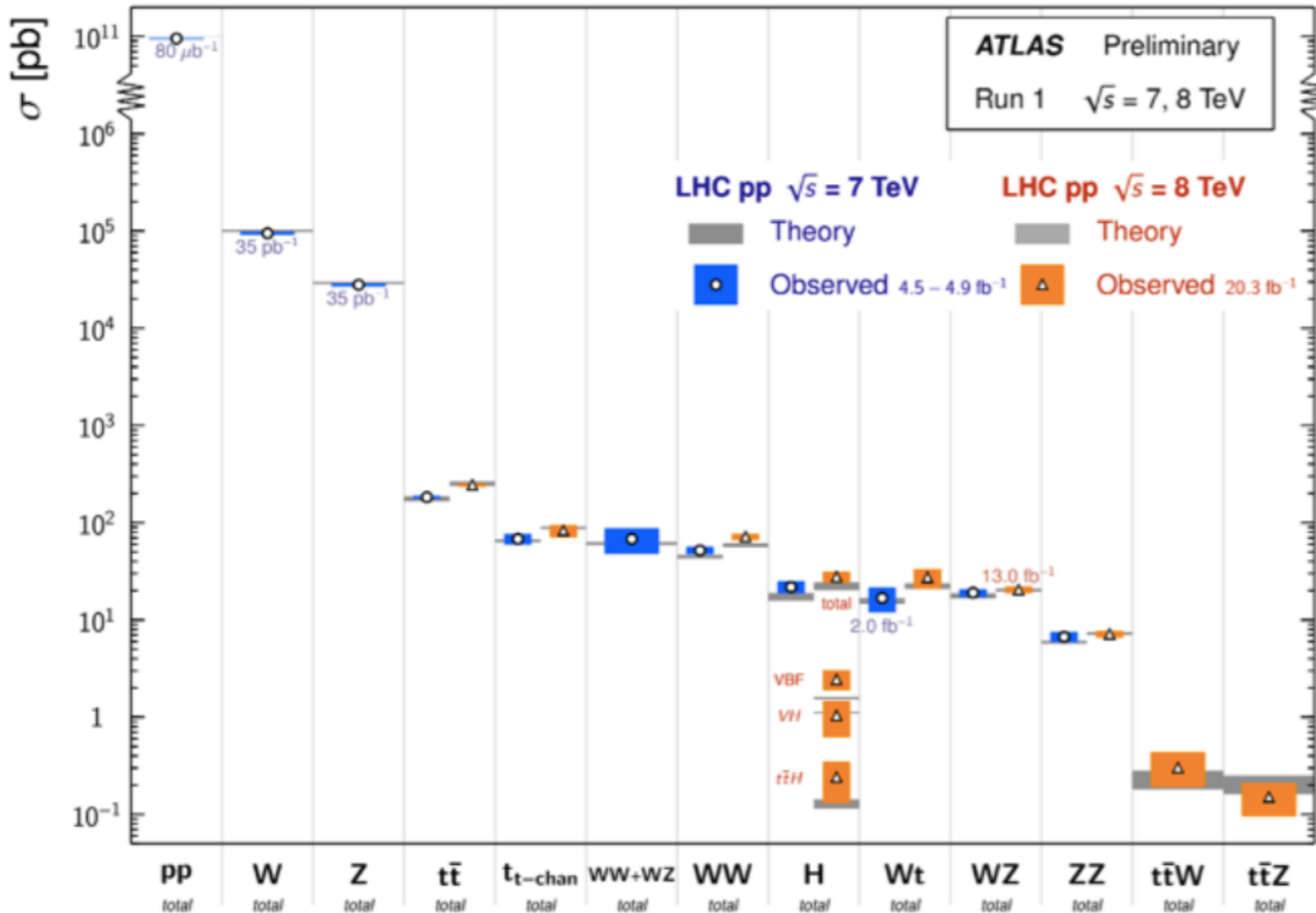
Table 2: Summary of event generators, showering programs and PDF sets used to model the Higgs boson production and decays at $\sqrt{s} = 8$ TeV.

Production process	Event generator	Showering program	PDF set
ggF	POWHEG	PYTHIA6/PYTHIA8	CT10
VBF	POWHEG	PYTHIA6/PYTHIA8	CT10
WH	PYTHIA8	PYTHIA8	CTEQ6L1
$ZH : q\bar{q} \rightarrow ZH$	PYTHIA8	PYTHIA8	CTEQ6L1
$ZH : gg \rightarrow ZH$	POWHEG	PYTHIA8	CT10
ttH	POWHEG	PYTHIA8	CT10
bbH	MADGRAPH5_AMC@NLO	HERWIG++	CT10
$tH : qb \rightarrow tHq'$	MADGRAPH	PYTHIA8	CT10
$tH : gb \rightarrow WtH$	MADGRAPH5_AMC@NLO	HERWIG++	CT10

Cross-sections of SM processes

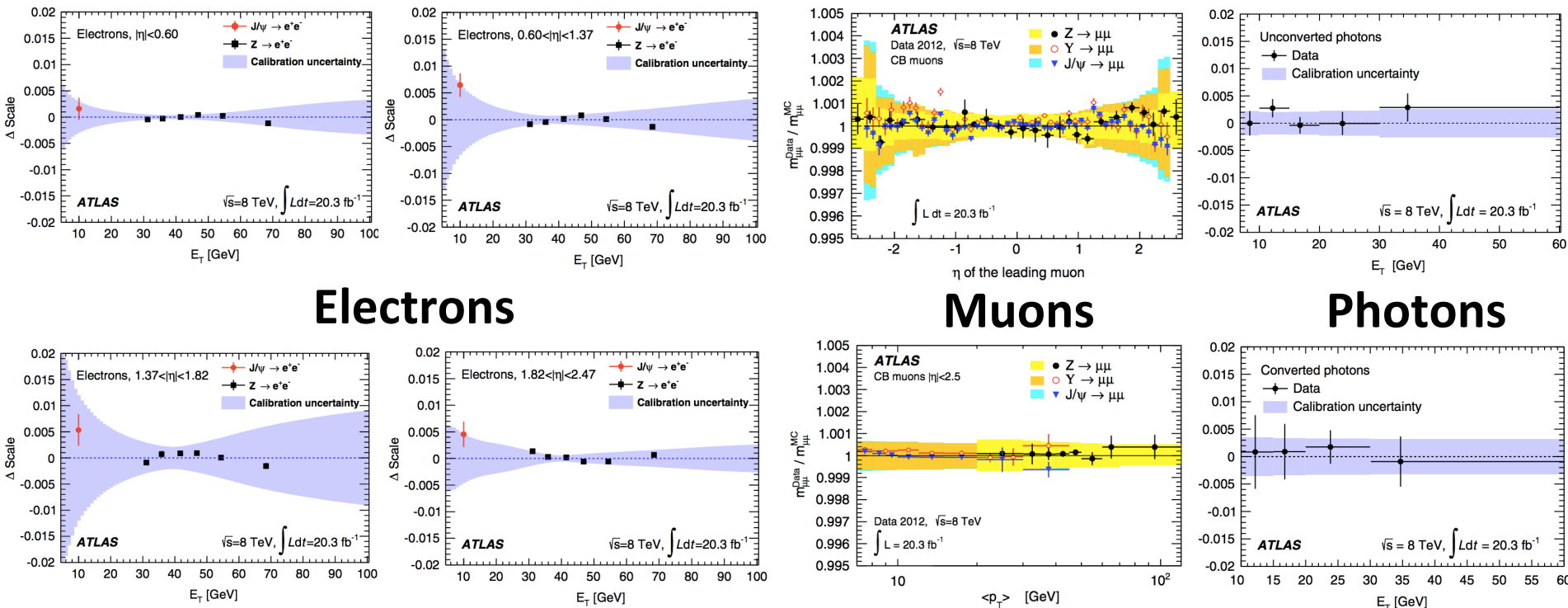
Standard Model Total Production Cross Section Measurements

Status: March 2015



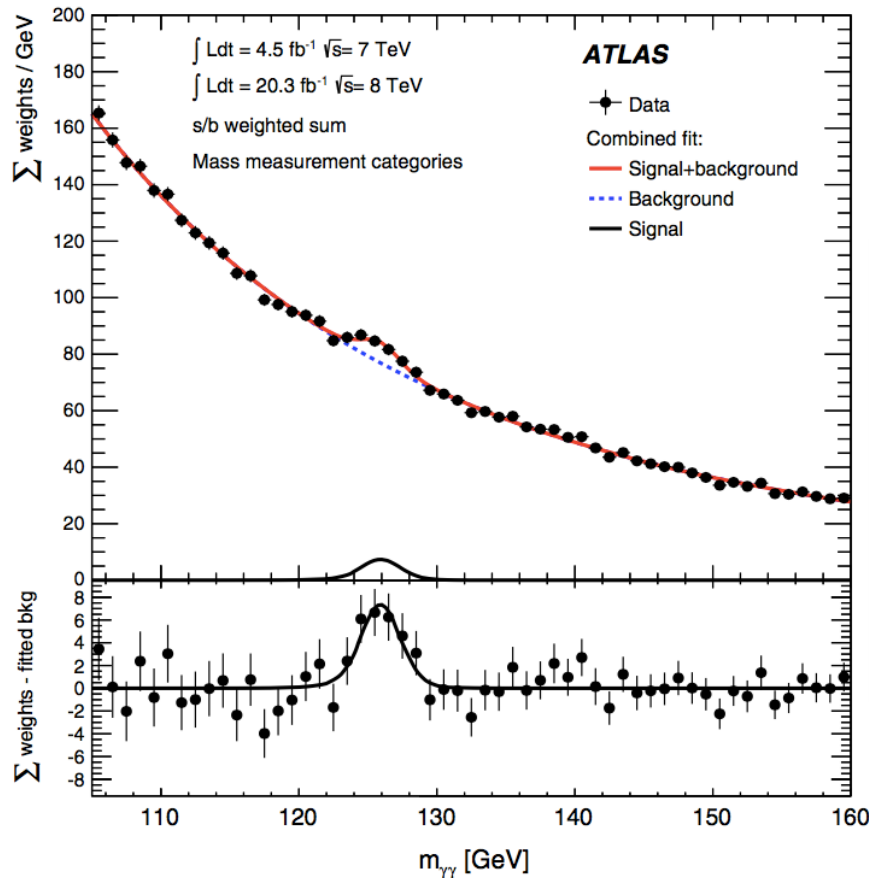
Calibration

Careful calibration of the transverse momentum/energy of the leptons and photons



[Phys. Rev. D. 90, 052004 \(2014\)](#)

m_H from $H \rightarrow \gamma\gamma$



- Data fit: exponential + **crystal ball**

$$N \cdot \begin{cases} e^{-t^2/2} & \text{if } t > -\alpha_{CB} \\ \left(\frac{n_{CB}}{\alpha_{CB}}\right)^{n_{CB}} e^{-\alpha_{CB}^2/2} \left(\frac{n_{CB}}{\alpha_{CB}} - \alpha_{CB} - t\right)^{-n_{CB}} & \text{otherwise} \end{cases}$$

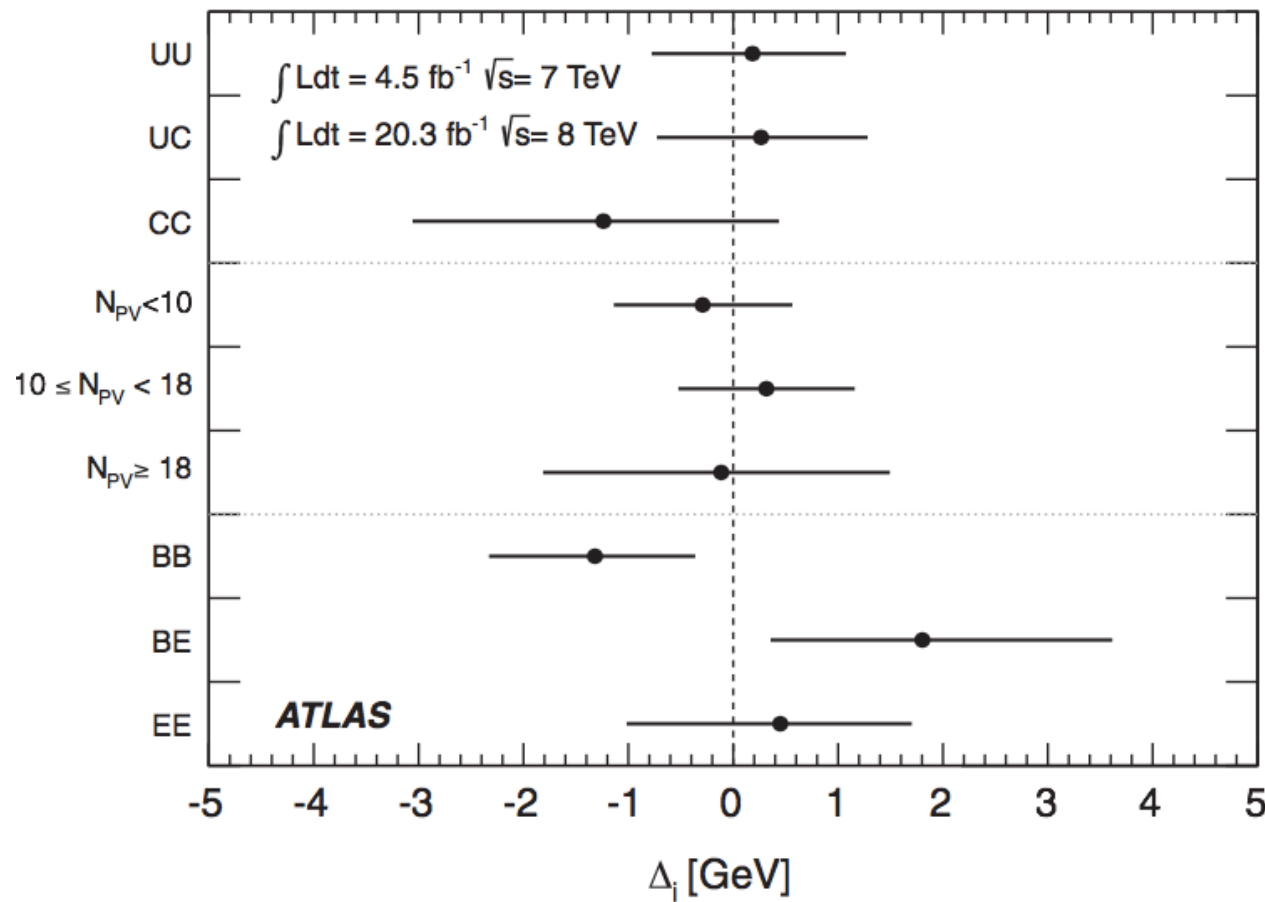
where $t = (m_{\gamma\gamma} - \mu_{CB})/\sigma_{CB}$, N is a normalization parameter, μ_{CB} is the peak of the narrow Gaussian distribution, σ_{CB} represents the Gaussian resolution for the core component, and n_{CB} and α_{CB} parametrize the non-Gaussian tail.

[Phys. Rev. D. 90, 052004 \(2014\)](#)

m_H from $H \rightarrow \gamma\gamma$

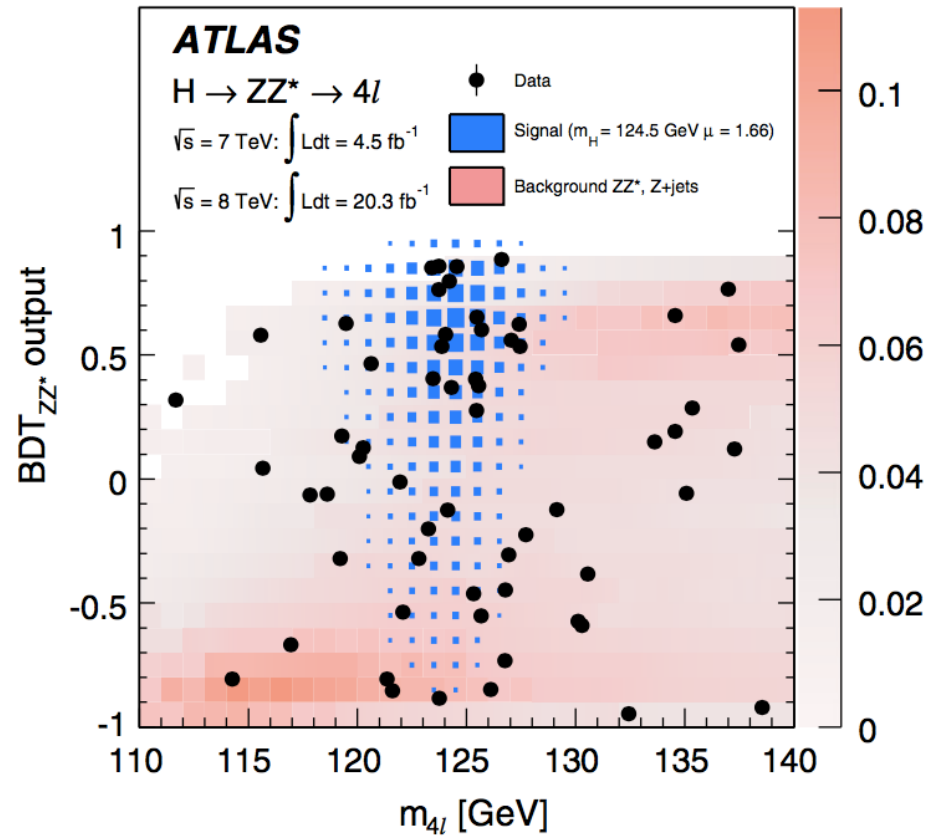
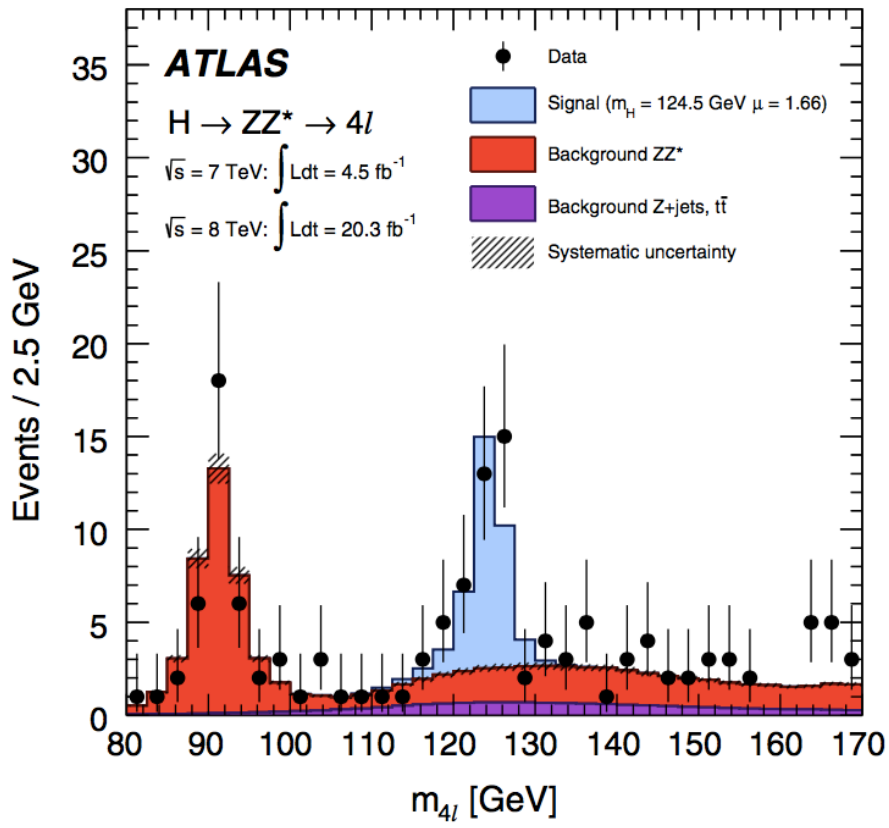
$$m_H = 125.98 \pm 0.42(\text{stat}) \pm 0.28(\text{syst}) \text{ GeV}$$
$$= 125.98 \pm 0.50 \text{ GeV}$$

[Phys. Rev. D. 90, 052004 \(2014\)](#)



m_H from $H \rightarrow ZZ^* \rightarrow 4l$

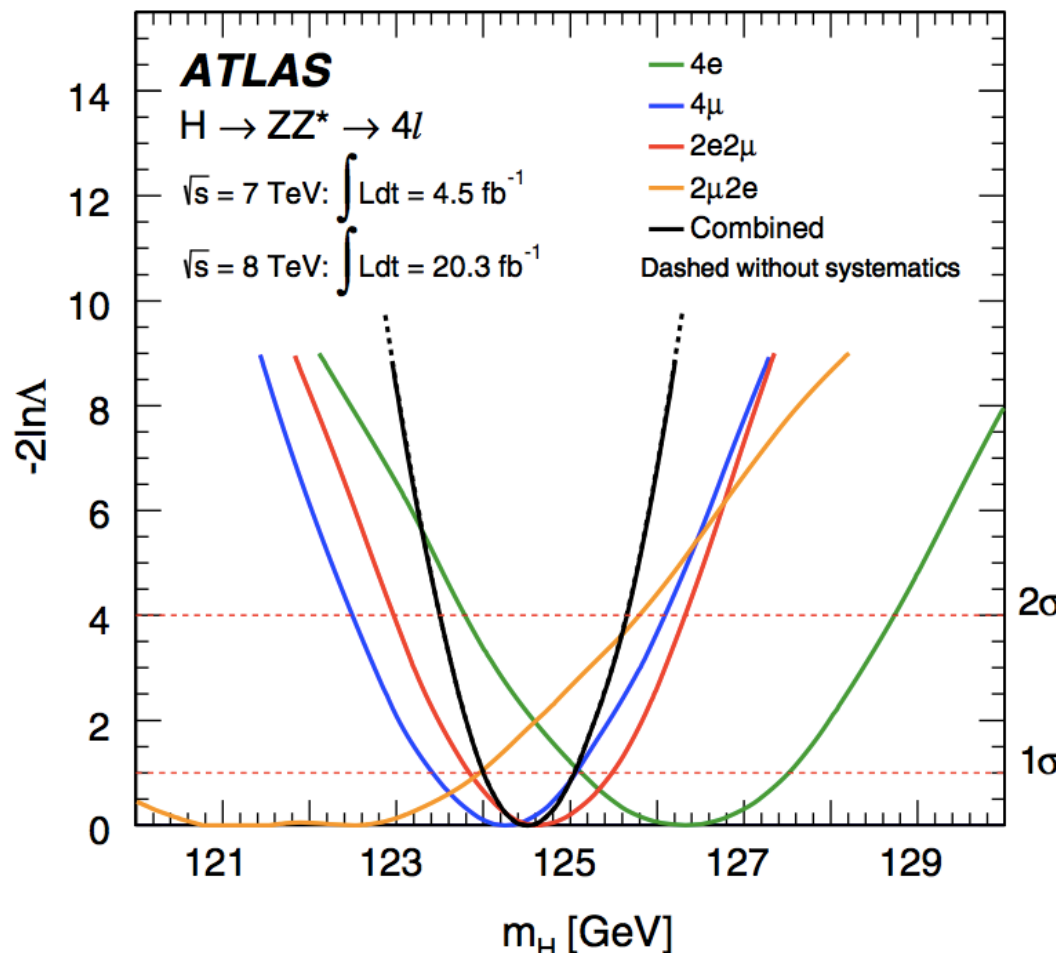
[Phys. Rev. D. 90, 052004 \(2014\)](#)



m_H from $H \rightarrow ZZ^* \rightarrow 4l$

$$m_H = 124.51 \pm 0.52(\text{stat}) \pm 0.06(\text{syst}) \text{ GeV}$$
$$= 124.51 \pm 0.52 \text{ GeV}$$

[Phys. Rev. D. 90, 052004 \(2014\)](#)



Combined m_H : systematics

Systematic	Uncertainty on m_H [MeV]
LAr syst on material before presampler (barrel)	70
LAr syst on material after presampler (barrel)	20
LAr cell nonlinearity (layer 2)	60
LAr cell nonlinearity (layer 1)	30
LAr layer calibration (barrel)	50
Lateral shower shape (conv)	50
Lateral shower shape (unconv)	40
Presampler energy scale (barrel)	20
ID material model ($ \eta < 1.1$)	50
$H \rightarrow \gamma\gamma$ background model (unconv rest low p_{Tt})	40
$Z \rightarrow ee$ calibration	50
Primary vertex effect on mass scale	20
Muon momentum scale	10
Remaining systematic uncertainties	70
Total	180

Coupling Channel Inputs (1)

arXiv:1507.04548 (2015)

Analysis	Signal		$\int \mathcal{L} dt [fb^{-1}]$	
	Strength μ	Significance [s.d.]	7 TeV	8 TeV
Categorisation or final states				
$H \rightarrow \gamma\gamma$ [12]	1.17 ± 0.27	5.2 (4.6)	4.5	20.3
ttH: leptonic, hadronic			✓	✓
VH: one-lepton, dilepton, E_T^{miss} , hadronic			✓	✓
VBF: tight, loose			✓	✓
ggF: 4 p_{Tt} categories			✓	✓
$H \rightarrow ZZ^* \rightarrow 4\ell$ [13]	$1.44^{+0.40}_{-0.33}$	8.1 (6.2)	4.5	20.3
VBF			✓	✓
VH: hadronic, leptonic			✓	✓
ggF			✓	✓
$H \rightarrow WW^*$ [14, 15]	$1.16^{+0.24}_{-0.21}$	6.5 (5.9)	4.5	20.3
ggF: (0-jet, 1-jet) \otimes ($ee + \mu\mu, e\mu$)			✓	✓
ggF: ≥ 2 -jet and $e\mu$				✓
VBF: ≥ 2 -jet \otimes ($ee + \mu\mu, e\mu$)			✓	✓
VH: opposite-charge dilepton, three-lepton, four-lepton			✓	✓
VH: same-charge dilepton				✓
$H \rightarrow \tau\tau$ [17]	$1.43^{+0.43}_{-0.37}$	4.5 (3.4)	4.5	20.3
Boosted: $\tau_{\text{lep}}\tau_{\text{lep}}, \tau_{\text{lep}}\tau_{\text{had}}, \tau_{\text{had}}\tau_{\text{had}}$			✓	✓
VBF: $\tau_{\text{lep}}\tau_{\text{lep}}, \tau_{\text{lep}}\tau_{\text{had}}, \tau_{\text{had}}\tau_{\text{had}}$			✓	✓
$VH \rightarrow Vb\bar{b}$ [18]	0.52 ± 0.40	1.4 (2.6)	4.7	20.3
0ℓ ($ZH \rightarrow vv b\bar{b}$): $N_{\text{jet}} = 2, 3, N_{\text{btag}} = 1, 2, p_T^V \in 100\text{-}120$ and > 120 GeV			✓	✓
1ℓ ($WH \rightarrow \ell v b\bar{b}$): $N_{\text{jet}} = 2, 3, N_{\text{btag}} = 1, 2, p_T^V <$ and > 120 GeV			✓	✓
2ℓ ($ZH \rightarrow \ell\ell b\bar{b}$): $N_{\text{jet}} = 2, 3, N_{\text{btag}} = 1, 2, p_T^V <$ and > 120 GeV			✓	✓

Coupling Channel Inputs (2)

[arXiv:1507.04548 \(2015\)](https://arxiv.org/abs/1507.04548)

95% CL limit			
$H \rightarrow Z\gamma$ [19]	$\mu < 11$ (9)	4.5	20.3
10 categories based on $\Delta\eta_{Z\gamma}$ and p_{Tt}		✓	✓
$H \rightarrow \mu\mu$ [20]	$\mu < 7.0$ (7.2)	4.5	20.3
VBF and 6 other categories based on η_μ and $p_T^{\mu\mu}$		✓	✓
$t\bar{t}H$ production [21–23]		4.5	20.3
$H \rightarrow b\bar{b}$: single-lepton, dilepton	$\mu < 3.4$ (2.2)		✓
$t\bar{t}H \rightarrow$ multileptons: categories on lepton multiplicity	$\mu < 4.7$ (2.4)		✓
$H \rightarrow \gamma\gamma$: leptonic, hadronic	$\mu < 6.7$ (4.9)	✓	✓
Off-shell H^* production [24]	$\mu < 5.1 - 8.6$ (6.7 – 11.0)		20.3
$H^* \rightarrow ZZ \rightarrow 4\ell$		✓	
$H^* \rightarrow ZZ \rightarrow 2\ell 2\nu$		✓	
$H^* \rightarrow WW \rightarrow e\nu\mu\nu$		✓	

Combined Signal Strength

[arXiv:1507.04548 \(2015\)](https://arxiv.org/abs/1507.04548)

$$\mu = 1.18^{+0.15}_{-0.14} = 1.18 \pm 0.10 \text{ (stat.)} \pm 0.07 \text{ (syst.)} {}^{+0.08}_{-0.07} \text{ (theo.)},$$

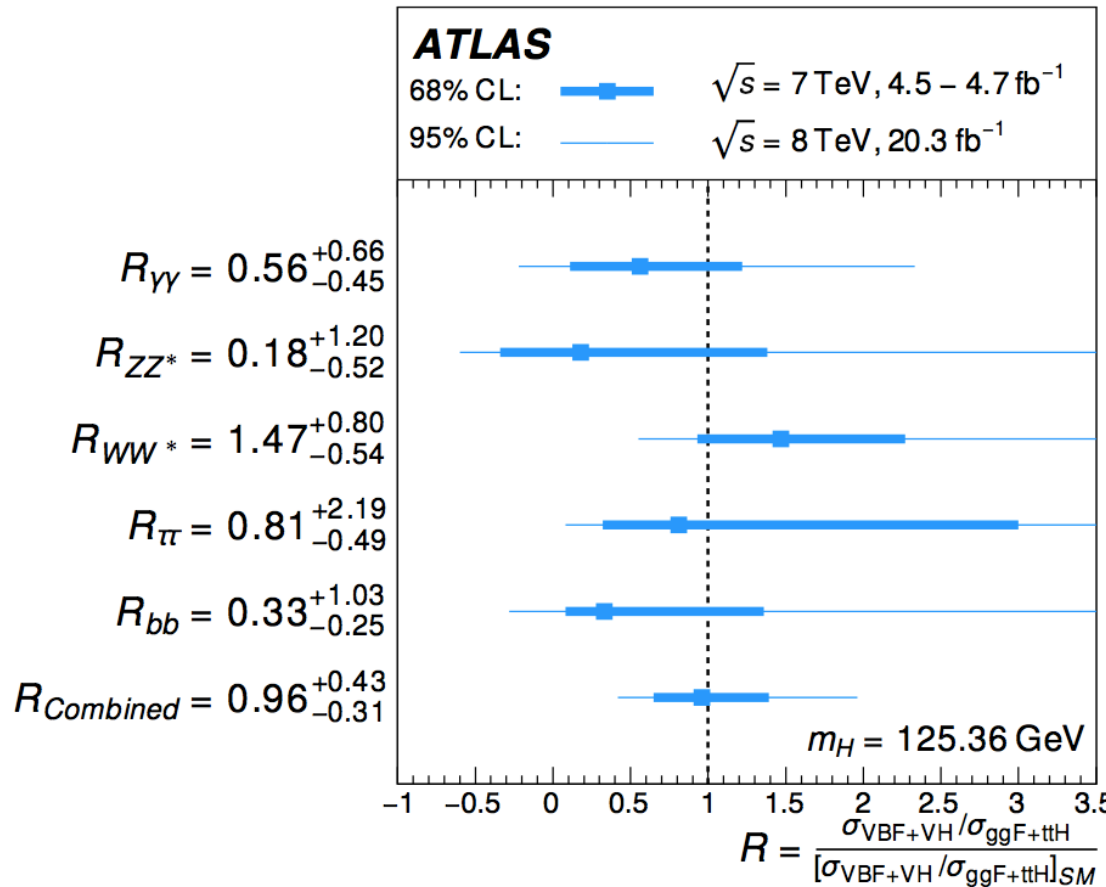
Production	Signal strength μ at $m_H = 125.36$ GeV					
process	$\sqrt{s} = 8$ TeV			Combined $\sqrt{s} = 7$ and 8 TeV		
ggF	$1.23^{+0.25}_{-0.21}$	$[+0.16 \quad +0.10 \quad +0.16]$	$[-0.16 \quad -0.08 \quad -0.11]$	$1.23^{+0.23}_{-0.20}$	$[+0.14 \quad +0.09 \quad +0.16]$	$[-0.14 \quad -0.08 \quad -0.12]$
VBF	$1.55^{+0.39}_{-0.35}$	$[+0.32 \quad +0.17 \quad +0.13]$	$[-0.31 \quad -0.13 \quad -0.11]$	1.23 ± 0.32	$[+0.28 \quad +0.13 \quad +0.11]$	$[-0.27 \quad -0.12 \quad -0.09]$
VH	0.93 ± 0.39	$[+0.37 \quad +0.20 \quad +0.12]$	$[-0.33 \quad -0.18 \quad -0.06]$	0.80 ± 0.36	$[+0.31 \quad +0.17 \quad +0.10]$	$[-0.30 \quad -0.17 \quad -0.05]$
ttH	1.62 ± 0.78	$[+0.51 \quad +0.58 \quad +0.28]$	$[-0.50 \quad -0.54 \quad -0.10]$	1.81 ± 0.80	$[+0.52 \quad +0.58 \quad +0.31]$	$[-0.50 \quad -0.55 \quad -0.12]$

Production process	Cross section [pb] at $\sqrt{s} = 8$ TeV		
ggF	23.9 ± 3.6	$[+3.1 \quad +1.9 \quad +1.0]$	$[-3.1 \quad -1.6 \quad -1.0]$
VBF	2.43 ± 0.58	$[+0.50 \quad +0.27 \quad +0.19]$	$[-0.49 \quad -0.20 \quad -0.16]$
VH	1.03 ± 0.53	$[+0.37 \quad +0.22 \quad +0.13]$	$[-0.36 \quad -0.20 \quad -0.06]$
ttH	0.24 ± 0.11	$[+0.07 \quad +0.08 \quad +0.01]$	$[-0.07 \quad -0.08 \quad -0.01]$

Combined Xsection Ratios

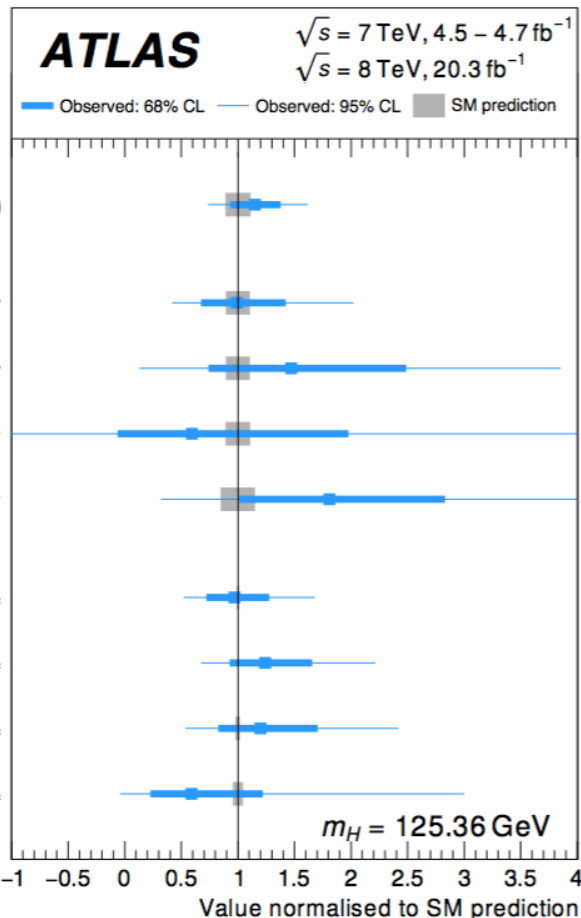
$$\frac{\mu_{\text{VBF+VH}}^f}{\mu_{\text{ggF+ttH}}^f} = \frac{\sigma_{\text{VBF+VH}}/\sigma_{\text{ggF+ttH}}}{[\sigma_{\text{VBF+VH}}/\sigma_{\text{ggF+ttH}}]_{\text{SM}}} = \frac{\mu_{\text{VBF+VH}}}{\mu_{\text{ggF+ttH}}} \equiv R_{ff} .$$

[arXiv:1507.04548 \(2015\)](https://arxiv.org/abs/1507.04548)



Combined Ratios of Production Xsections and Partial Decay Widths

$$\sigma_i \cdot \text{BR}_f = \left(\sigma_{\text{ggF}} \cdot \text{BR}_{WW^*} \right) \times \left(\frac{\sigma_i}{\sigma_{\text{ggF}}} \right) \times \left(\frac{\text{BR}_f}{\text{BR}_{WW^*}} \right) = \sigma(gg \rightarrow H \rightarrow WW^*) \times \left(\frac{\sigma_i}{\sigma_{\text{ggF}}} \right) \times \left(\frac{\Gamma_f}{\Gamma_{WW^*}} \right).$$



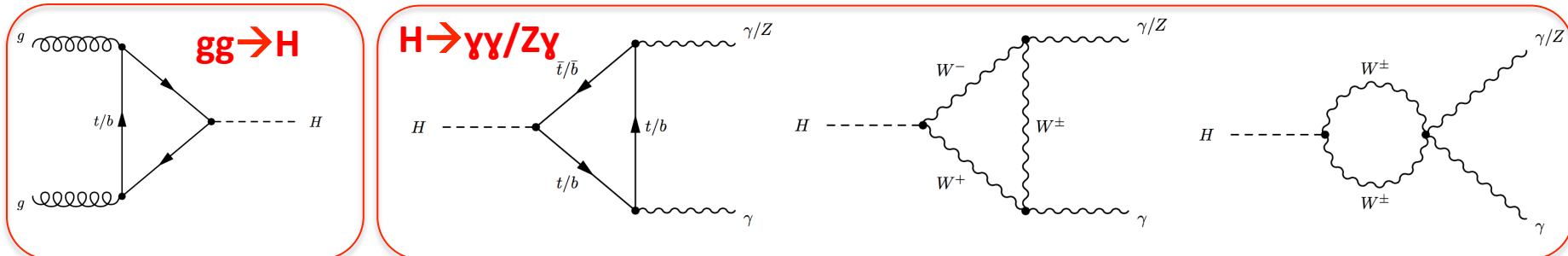
[arXiv:1507.04548 \(2015\)](https://arxiv.org/abs/1507.04548)

- Observed and expected significances in units of standard deviations, for the rarer Higgs-productions modes:

Process	VBF	$t\bar{t}H$	WH	ZH	VH
Observed	4.3	2.5	2.1	0.9	2.6
Expected	3.8	1.5	2.0	2.1	3.1

Effective Couplings

- In some of the fits, scale factors κ_g , κ_γ and $\kappa_{Z\gamma}$ are introduced for loop-induced processes:



- We can write the effective scale factors as a function of the fundamental ones.

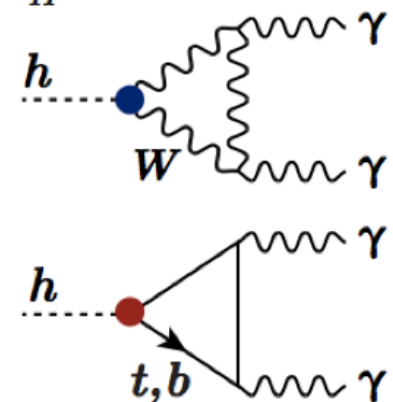
For example:

$$\sigma \mathcal{B}(gg \rightarrow H \rightarrow \gamma\gamma) = (\sigma_{ggF} \mathcal{B})_{SM}(gg \rightarrow H \rightarrow \gamma\gamma) \times \frac{\kappa_g^2 \kappa_\gamma^2}{\kappa_H^2}$$

where κ_g and κ_γ are effective multipliers since the Higgs boson does not directly couple to these particles, but via loops that contains interference:

$$\kappa_\gamma^2 = 1.59 \kappa_W^2 - 0.66 \kappa_W \kappa_t + 0.07 \kappa_t^2$$

these relations are modified if non-SM particles enter the loop



Coupling multipliers (1)

To a very good approximation, the relevant expressions for $m_H = 125.5$ GeV are:

$$\kappa_\gamma^2 \sim 1.59 \cdot \kappa_W^2 - 0.66 \cdot \kappa_W \kappa_t + 0.07 \cdot \kappa_t^2$$

$$\kappa_g^2 \sim 1.06 \cdot \kappa_t^2 - 0.07 \cdot \kappa_t \kappa_b + 0.01 \cdot \kappa_b^2$$

$$\kappa_{\text{VBF}}^2 \sim 0.74 \cdot \kappa_W^2 + 0.26 \cdot \kappa_Z^2$$

$$\kappa_H^2 \sim 0.57 \cdot \kappa_b^2 + 0.22 \cdot \kappa_W^2 + 0.09 \cdot \kappa_g^2 + 0.06 \cdot \kappa_\tau^2 + 0.03 \cdot \kappa_Z^2 + 0.03 \cdot \kappa_c^2.$$

- **Note:** The interference terms allows to check the sign of the couplings multipliers κ

Coupling multipliers (2)

arXiv:1507.04548 (2015)

Production	Loops	Interference	Expression in fundamental coupling-strength scale factors		
$\sigma(\text{ggF})$	✓	$b-t$	$\kappa_g^2 \sim$	$1.06 \cdot \kappa_t^2 + 0.01 \cdot \kappa_b^2 - 0.07 \cdot \kappa_t \kappa_b$	
$\sigma(\text{VBF})$	-	-	\sim	$0.74 \cdot \kappa_W^2 + 0.26 \cdot \kappa_Z^2$	
$\sigma(WH)$	-	-	\sim	κ_W^2	
$\sigma(q\bar{q} \rightarrow ZH)$	-	-	\sim	κ_Z^2	
$\sigma(gg \rightarrow ZH)$	✓	$Z-t$	$\kappa_{ggZH}^2 \sim$	$2.27 \cdot \kappa_Z^2 + 0.37 \cdot \kappa_t^2 - 1.64 \cdot \kappa_Z \kappa_t$	
$\sigma(bbH)$	-	-	\sim	κ_b^2	
$\sigma(ttH)$	-	-	\sim	κ_t^2	
$\sigma(gb \rightarrow WtH)$	-	$W-t$	\sim	$1.84 \cdot \kappa_t^2 + 1.57 \cdot \kappa_W^2 - 2.41 \cdot \kappa_t \kappa_W$	
$\sigma(qb \rightarrow tHq')$	-	$W-t$	\sim	$3.4 \cdot \kappa_t^2 + 3.56 \cdot \kappa_W^2 - 5.96 \cdot \kappa_t \kappa_W$	
Partial decay width					
$\Gamma_{b\bar{b}}$	-	-	\sim	κ_b^2	
Γ_{WW}	-	-	\sim	κ_W^2	
Γ_{ZZ}	-	-	\sim	κ_Z^2	
$\Gamma_{\tau\tau}$	-	-	\sim	κ_τ^2	
$\Gamma_{\mu\mu}$	-	-	\sim	κ_μ^2	
$\Gamma_{\gamma\gamma}$	✓	$W-t$	$\kappa_\gamma^2 \sim$	$1.59 \cdot \kappa_W^2 + 0.07 \cdot \kappa_t^2 - 0.66 \cdot \kappa_W \kappa_t$	
$\Gamma_{Z\gamma}$	✓	$W-t$	$\kappa_{Z\gamma}^2 \sim$	$1.12 \cdot \kappa_W^2 + 0.00035 \cdot \kappa_t^2 - 0.12 \cdot \kappa_W \kappa_t$	
Total decay width					
Γ_H	✓	$W-t$ $b-t$	$\kappa_H^2 \sim$	$0.57 \cdot \kappa_b^2 + 0.22 \cdot \kappa_W^2 + 0.09 \cdot \kappa_g^2 +$ $0.06 \cdot \kappa_\tau^2 + 0.03 \cdot \kappa_Z^2 + 0.03 \cdot \kappa_c^2 +$ $0.0023 \cdot \kappa_\gamma^2 + 0.0016 \cdot \kappa_{Z\gamma}^2 + 0.00022 \cdot \kappa_\mu^2$	

Benchmark Coupling Models

- Many test are possible, under different assumptions:
 - Allow/don't allow invisible decays (contribution to total width)
 - Allow/don't allow BSM particles in loops

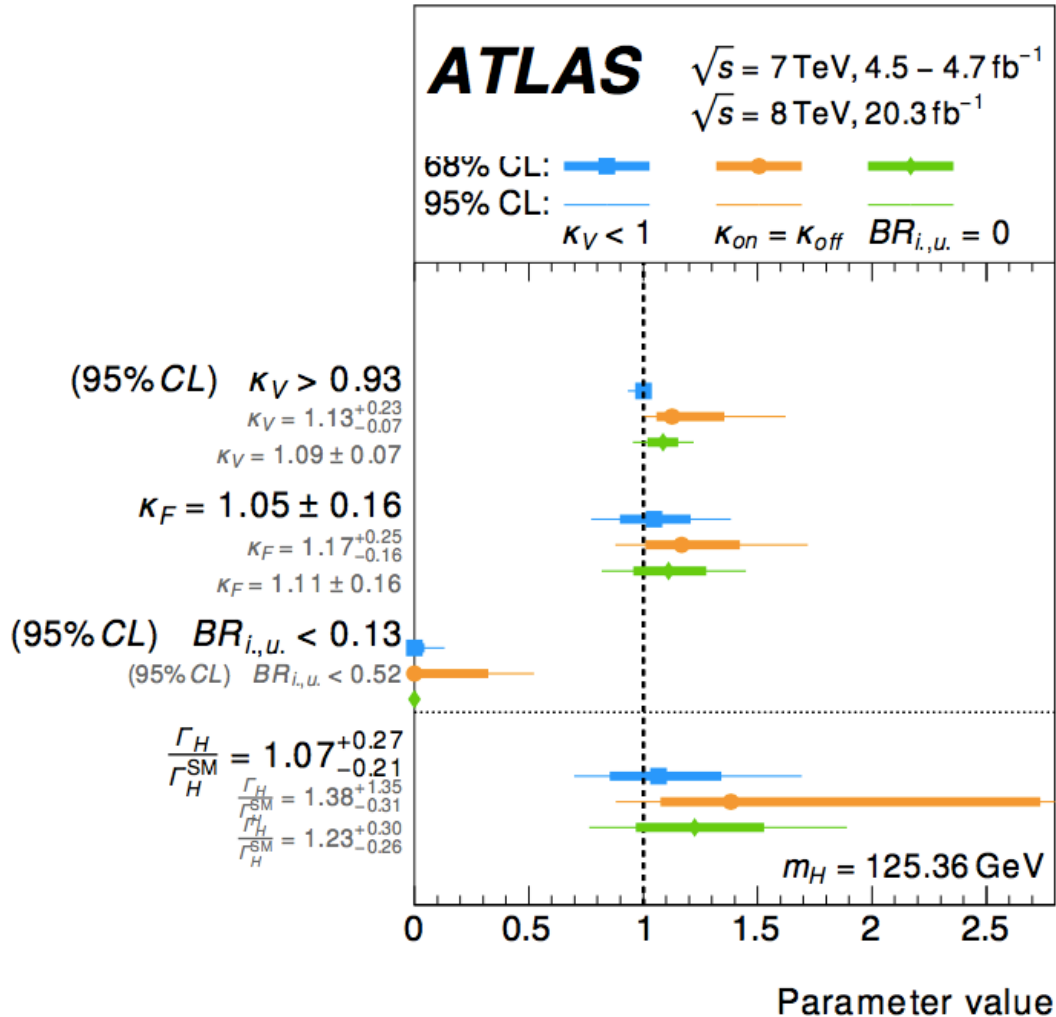
[arXiv:1507.04548 \(2015\)](https://arxiv.org/abs/1507.04548)

Table 10: Summary of benchmark coupling models considered in this paper, where $\lambda_{ij} \equiv \kappa_i/\kappa_j$, $\kappa_{ii} \equiv \kappa_i\kappa_i/\kappa_H$, and the functional dependence assumptions are: $\kappa_V = \kappa_W = \kappa_Z$, $\kappa_F = \kappa_t = \kappa_b = \kappa_\tau = \kappa_\mu$ (and similarly for the other fermions), $\kappa_g = \kappa_g(\kappa_b, \kappa_t)$, $\kappa_\gamma = \kappa_\gamma(\kappa_b, \kappa_t, \kappa_\tau, \kappa_W)$, and $\kappa_H = \kappa_H(\kappa_i)$. The tick marks indicate which assumptions are made in each case. The last column shows, as an example, the relative coupling strengths involved in the $gg \rightarrow H \rightarrow \gamma\gamma$ process.

Section in this paper	Corresponding table in Ref.[11]	Probed couplings	Parameters of interest	Functional assumptions					Example: $gg \rightarrow H \rightarrow \gamma\gamma$
				κ_V	κ_F	κ_g	κ_γ	κ_H	
5.2.1	43.1	Couplings to fermions and bosons	κ_V, κ_F	✓	✓	✓	✓	✓	$\kappa_F^2 \cdot \kappa_\gamma^2(\kappa_F, \kappa_V)/\kappa_H^2(\kappa_F, \kappa_V)$
5.2.2	43.2		$\kappa_F, \kappa_V, \text{BR}_{i,u.}$	≤ 1	—	✓	✓	✓	$\frac{\kappa_F^2 \cdot \kappa_\gamma(\kappa_F, \kappa_V)^2}{\kappa_H^2(\kappa_F, \kappa_V)} \cdot (1 - \text{BR}_{i,u.})$
5.2.3	43.3		$\lambda_{FV}, \kappa_{VV}$	✓	✓	✓	✓	—	$\kappa_{VV}^2 \cdot \lambda_{FV}^2 \cdot \kappa_\gamma^2(\lambda_{FV}, \lambda_{FV}, \lambda_{FV}, 1)$
5.3.1	46	Up-/down-type fermions	$\lambda_{du}, \lambda_{Vu}, \kappa_{uu}$	✓	κ_u, κ_d	✓	✓	—	$\kappa_{uu}^2 \cdot \kappa_g^2(\lambda_{du}, 1) \cdot \kappa_\gamma^2(\lambda_{du}, 1, \lambda_{du}, \lambda_{Vu})$
5.3.2	47	Leptons/quarks	$\lambda_{\ell q}, \lambda_{Vq}, \kappa_{qq}$	✓	κ_ℓ, κ_q	✓	✓	—	$\kappa_{qq}^2 \cdot \kappa_\gamma^2(1, 1, \lambda_{\ell q}, \lambda_{Vq})$
5.4.1	48.1	Vertex loops + $H \rightarrow$ invisible/undetected decays	$\kappa_g, \kappa_\gamma, \kappa_{Z\gamma}$	=1	=1	—	—	✓	$\kappa_g^2 \cdot \kappa_\gamma^2/\kappa_H^2(\kappa_g, \kappa_\gamma)$
5.4.2	48.2		$\kappa_g, \kappa_\gamma, \kappa_{Z\gamma}, \text{BR}_{i,u.}$	=1	=1	—	—	✓	$\kappa_g^2 \cdot \kappa_\gamma^2/\kappa_H^2(\kappa_g, \kappa_\gamma) \cdot (1 - \text{BR}_{i,u.})$
5.4.3	49		$\kappa_F, \kappa_V, \kappa_g, \kappa_\gamma, \kappa_{Z\gamma}, \text{BR}_{i,u.}$	≤ 1	—	—	—	✓	$\frac{\kappa_F^2 \cdot \kappa_\gamma(\kappa_F, \kappa_V)^2}{\kappa_H^2(\kappa_F, \kappa_V, \kappa_g, \kappa_\gamma)} \cdot (1 - \text{BR}_{i,u.})$
5.5.1	51	Generic models with and without assumptions on vertex loops and Γ_H	$\kappa_W, \kappa_Z, \kappa_t, \kappa_b, \kappa_\tau, \kappa_\mu$	—	—	✓	✓	✓	$\frac{\kappa_g^2(\kappa_b, \kappa_t) \cdot \kappa_\gamma^2(\kappa_b, \kappa_t, \kappa_\tau, \kappa_\mu, \kappa_W)}{\kappa_H^2(\kappa_b, \kappa_t, \kappa_\tau, \kappa_\mu, \kappa_W, \kappa_Z)}$
5.5.2	50.2		$\kappa_W, \kappa_Z, \kappa_t, \kappa_b, \kappa_\tau, \kappa_\mu, \kappa_g, \kappa_\gamma, \kappa_{Z\gamma}, \text{BR}_{i,u.}$	≤ 1	—	—	—	✓	$\frac{\kappa_g^2 \cdot \kappa_\gamma^2}{\kappa_H^2(\kappa_b, \kappa_t, \kappa_\tau, \kappa_\mu, \kappa_W, \kappa_Z)} \cdot (1 - \text{BR}_{i,u.})$
5.5.3	50.3		$\lambda_{WZ}, \lambda_{tg}, \lambda_{bZ}, \lambda_{\tau Z}, \lambda_{gZ}, \lambda_{\gamma Z}, \lambda_{(Z\gamma)Z}, \kappa_{gZ}$	—	—	—	—	—	$\kappa_{gZ}^2 \cdot \lambda_{\gamma Z}^2$

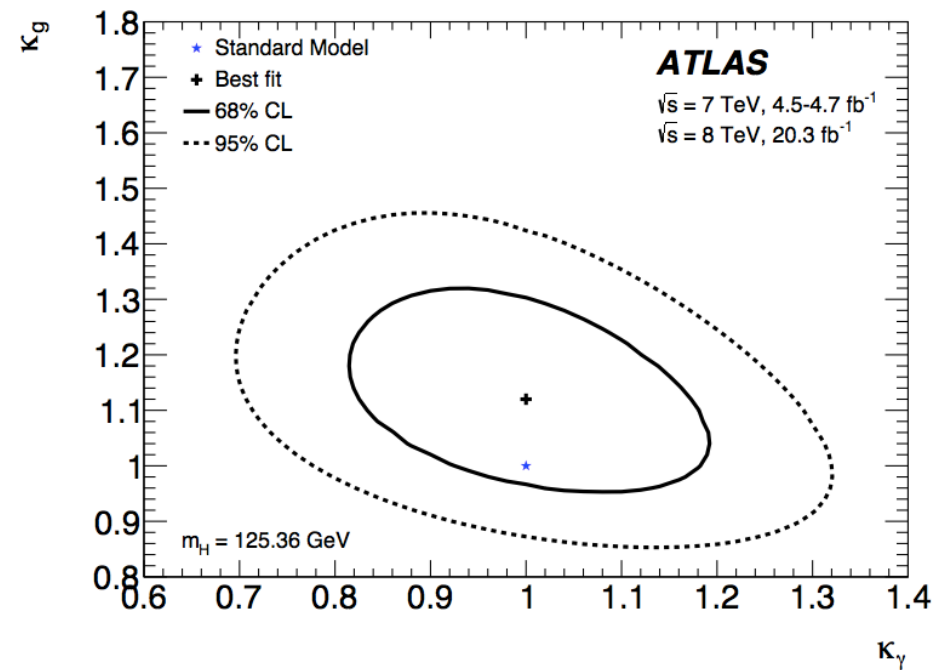
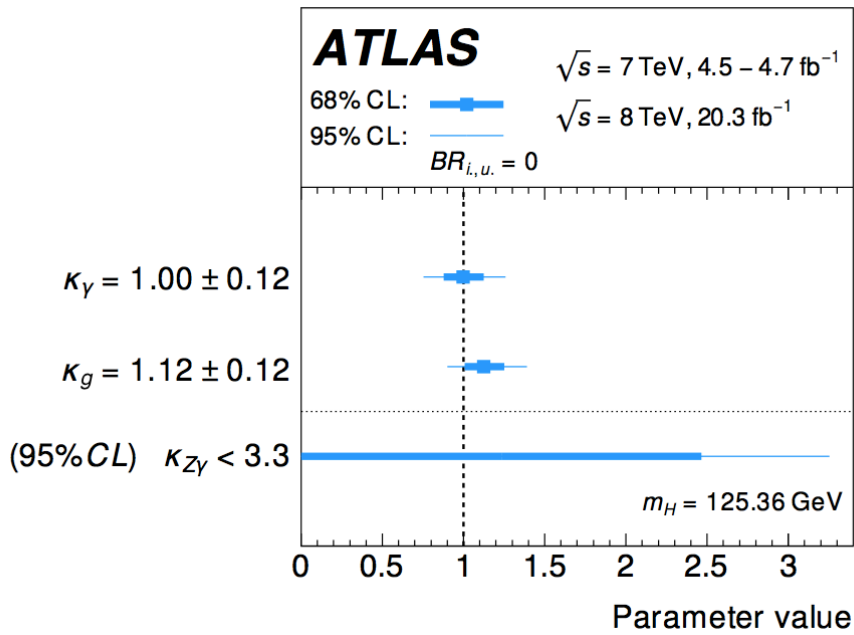
Probing BSM contributions (1)

- Benchmark model that probes for potential extra contributions to the total width, but does not allow contributions of non-SM particles in the loops



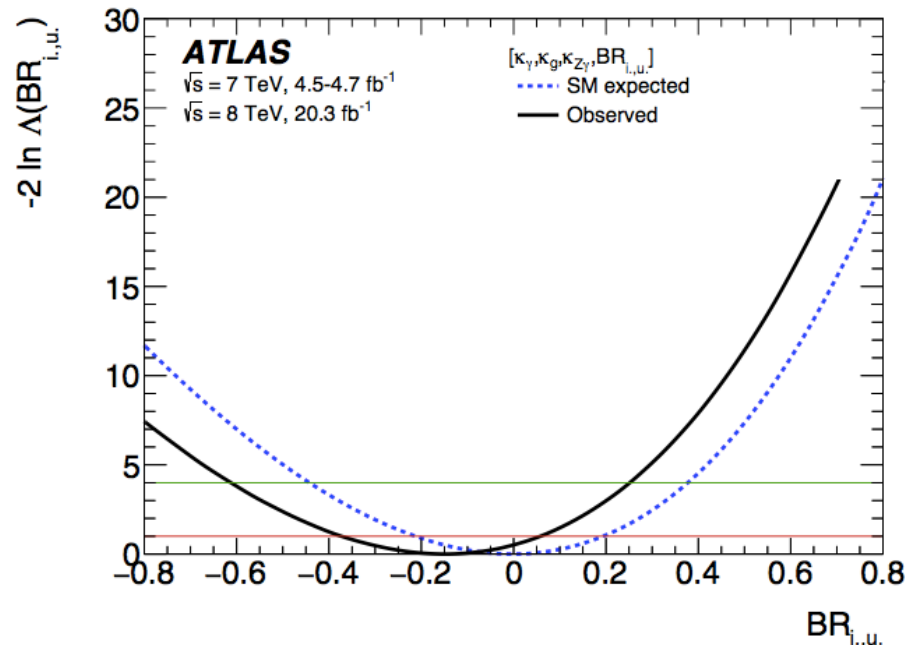
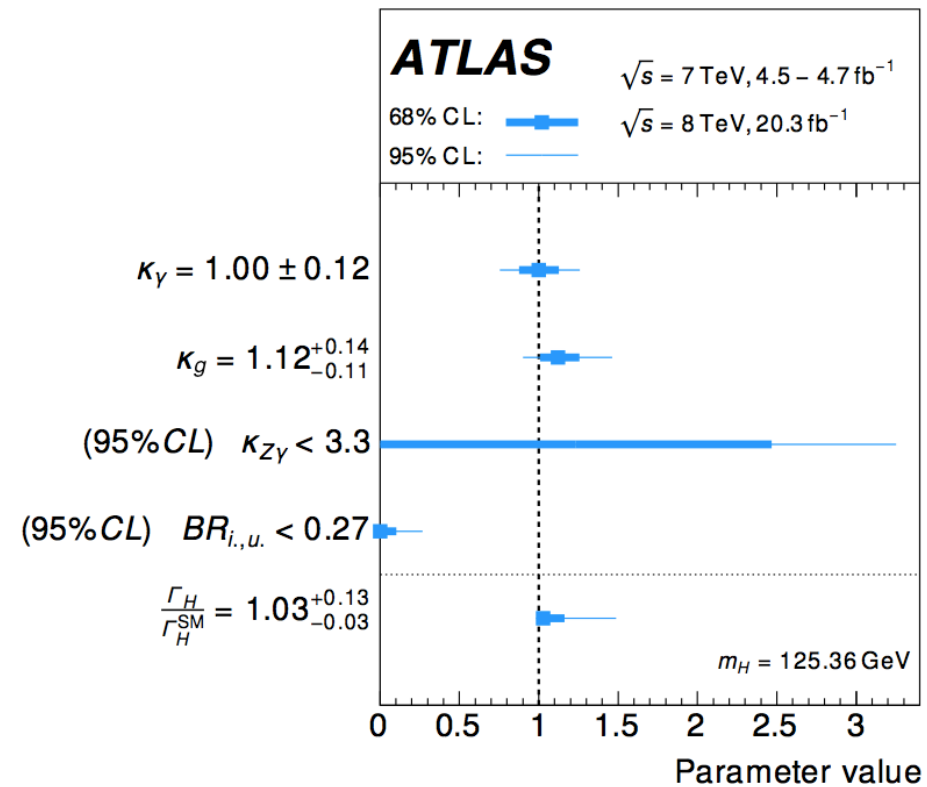
Probing BSM contributions (2)

- Benchmark model that probes for potential extra contributions to loops from non-SM particles, but does not allow contributions to total width



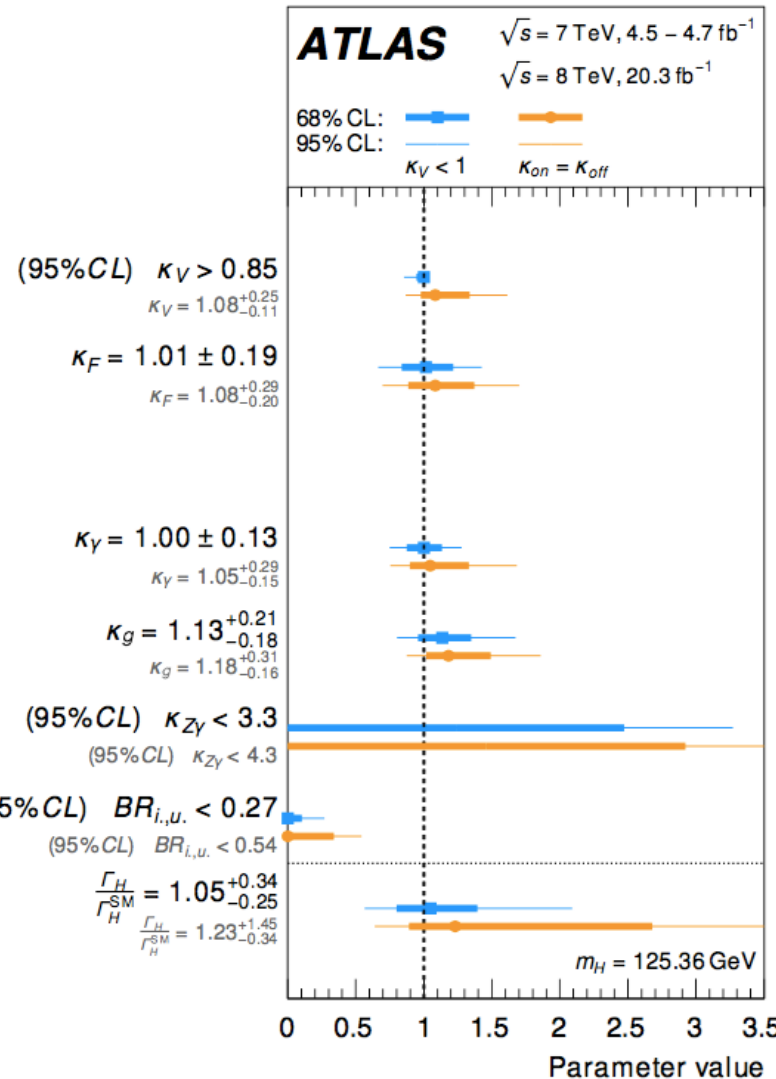
Probing BSM contributions (3)

- Benchmark model that probes for potential extra contributions to both loops and total width from non-SM particles



Probing BSM contributions (4)

- Benchmark model where non-BSM particles can contribute to both loops and total width, and remove assumption of SM couplings of Higgs for non-loop vertices (κ_V , κ_F)

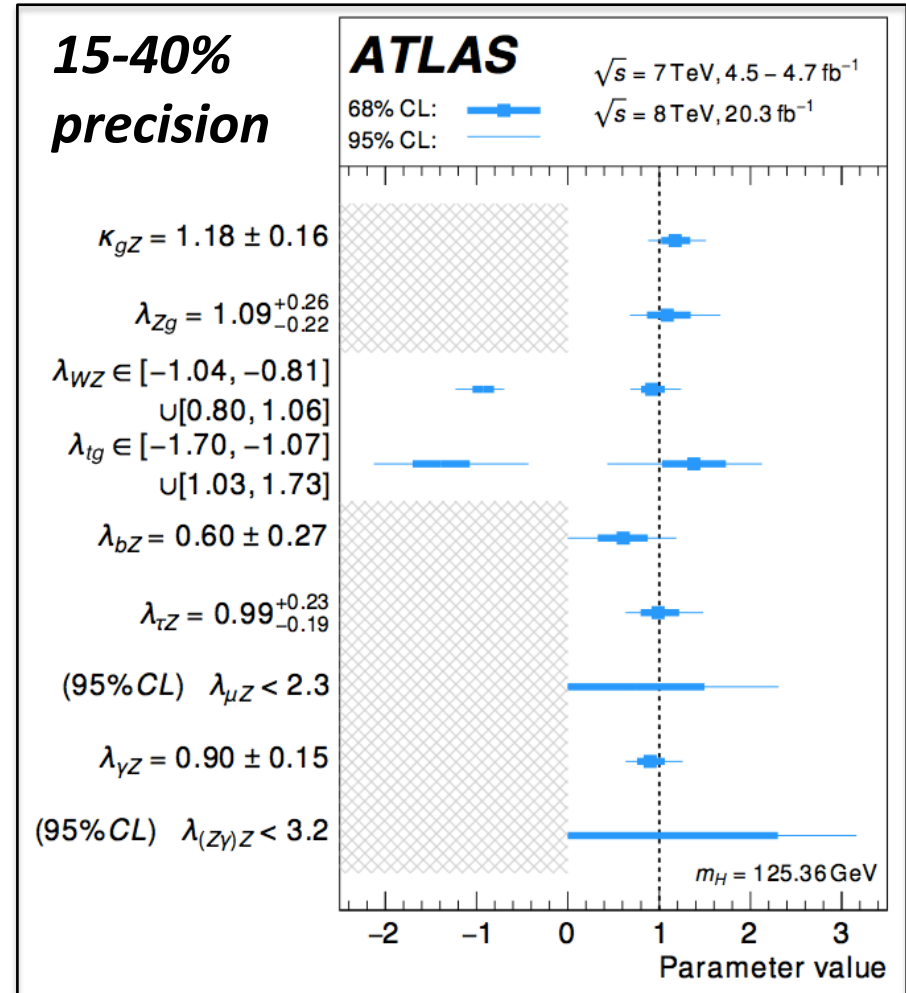
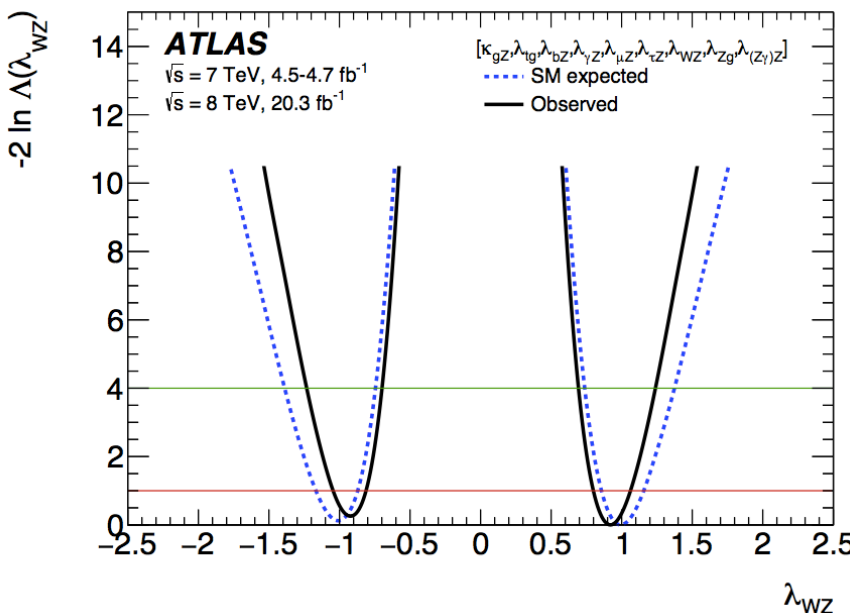


Most Generic Coupling Model

- In previous results, coupling multipliers were combined into a minimum number of parameters under certain assumptions. **In the generic models, the couplings strengths are treated independently.**

$$\begin{aligned}
 \kappa_{gZ} &= \kappa_g \cdot \kappa_Z / \kappa_H & \lambda_{\tau Z} &= \kappa_\tau / \kappa_Z \\
 \lambda_{Zg} &= \kappa_Z / \kappa_g & \lambda_{\mu Z} &= \kappa_\mu / \kappa_Z \\
 \lambda_{WZ} &= \kappa_W / \kappa_Z & \lambda_{\gamma Z} &= \kappa_\gamma / \kappa_Z \\
 \lambda_{tg} &= \kappa_t / \kappa_g & \lambda_{(Z\gamma)Z} &= \kappa_{Z\gamma} / \kappa_Z \\
 \lambda_{bZ} &= \kappa_b / \kappa_Z
 \end{aligned}$$

- Moreover, **allow BSM particles in loops**, and **make no assumption on total width**.



[arXiv:1507.04548 \(2015\)](https://arxiv.org/abs/1507.04548)

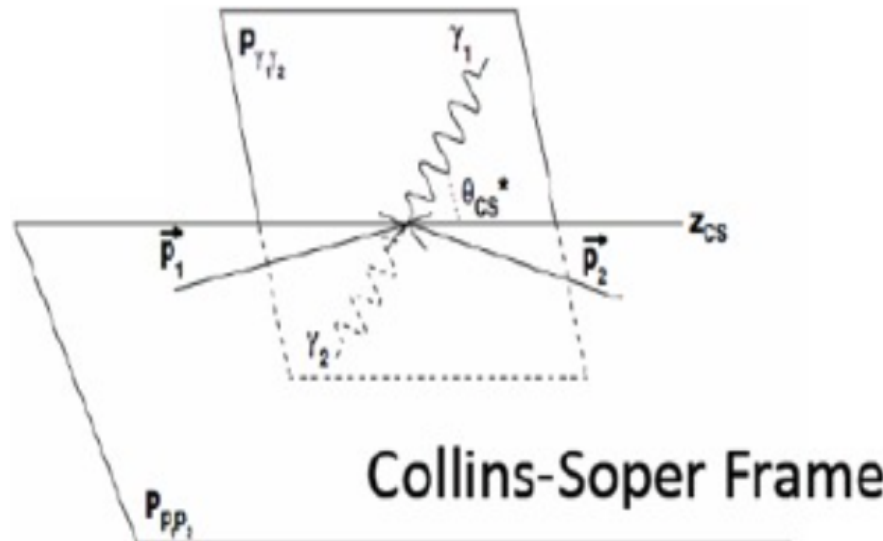
Collins-Soper Frame

Kinematic variables sensitive to the spin of the resonance are the diphoton transverse momentum $p_T^{\gamma\gamma}$ and the production angle of the two photons, measured in the Collins–Soper frame [33]:

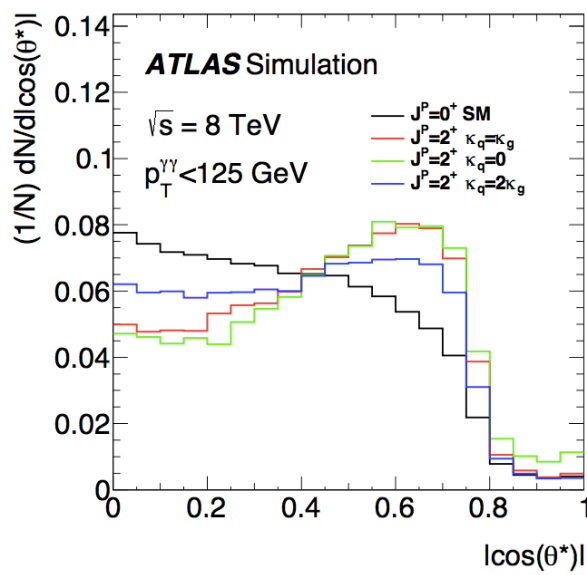
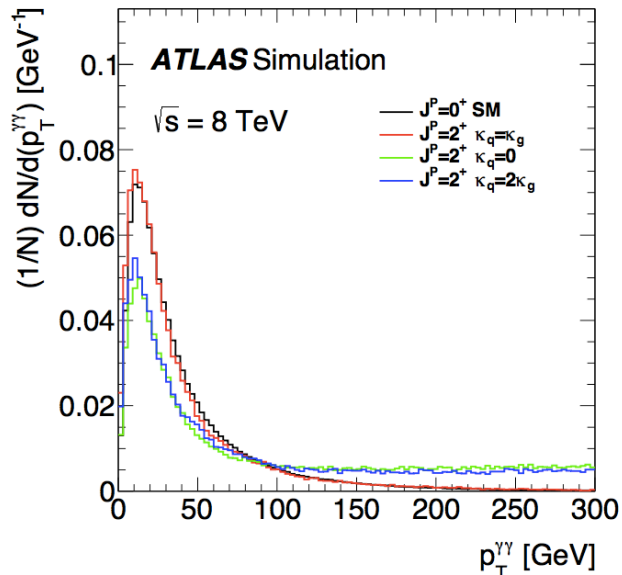
$$|\cos \theta^*| = \frac{|\sinh(\Delta\eta^{\gamma\gamma})|}{\sqrt{1 + (p_T^{\gamma\gamma}/m_{\gamma\gamma})^2}} \frac{2p_T^{\gamma_1} p_T^{\gamma_2}}{m_{\gamma\gamma}^2}, \quad (7)$$

where $\Delta\eta^{\gamma\gamma}$ is the separation in pseudorapidity of the two photons.

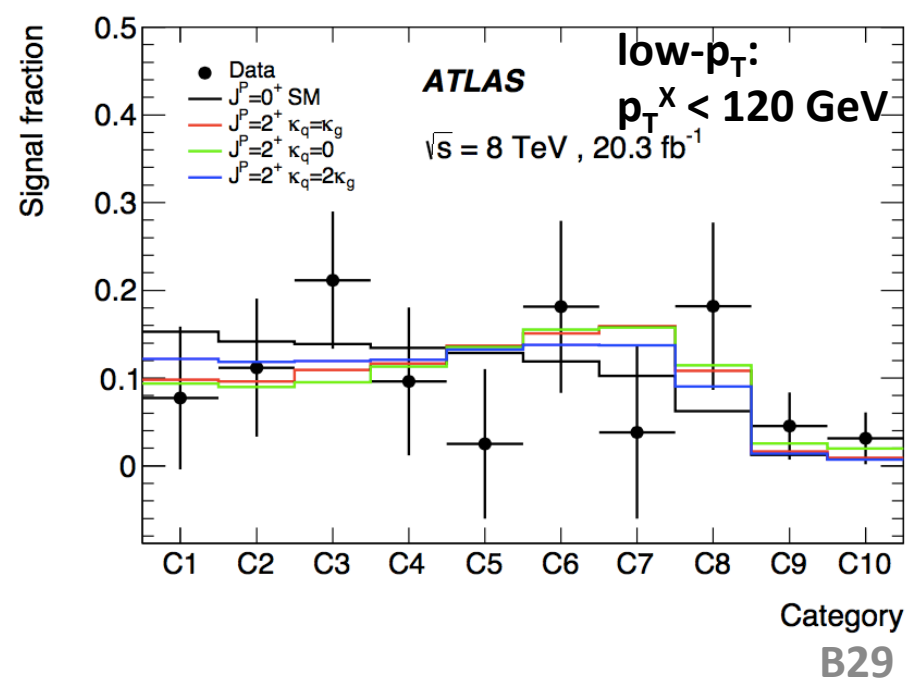
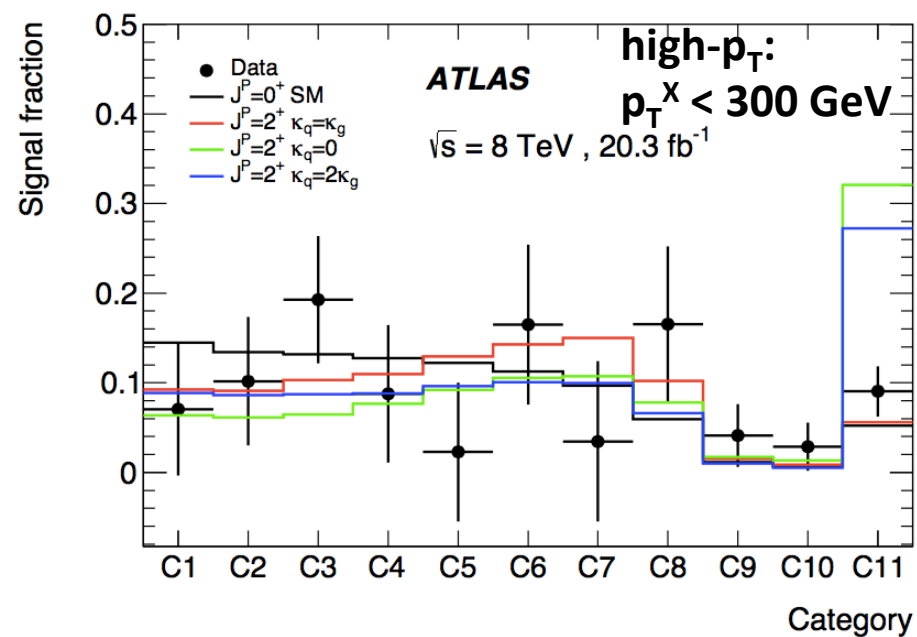
- Boosting to the Higgs rest frame, and then rotating in such a way that the measured variables remain sensitive to spin and CP properties of the Higgs.



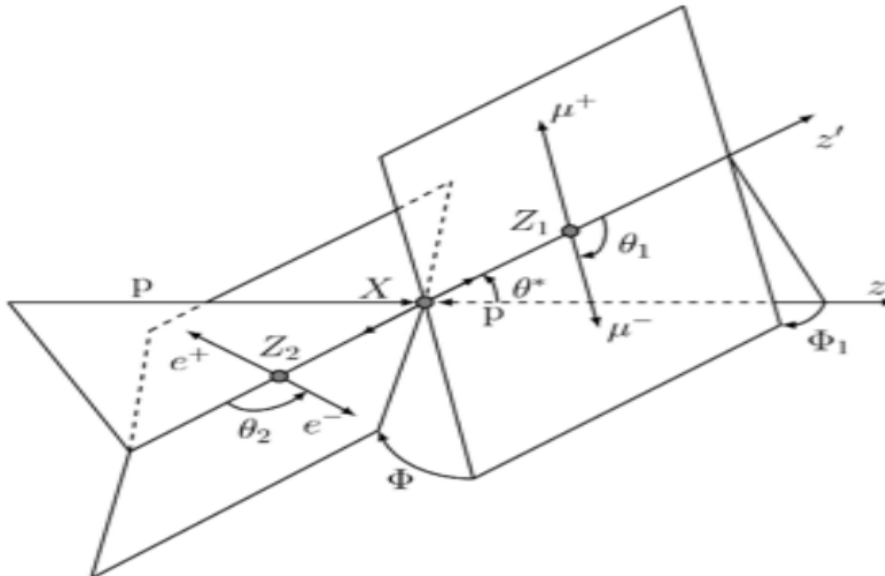
Spin from $H \rightarrow \gamma\gamma$



[arXiv:1506.05669 \(2015\)](https://arxiv.org/abs/1506.05669)



$H \rightarrow ZZ^* \rightarrow 4l$ decay

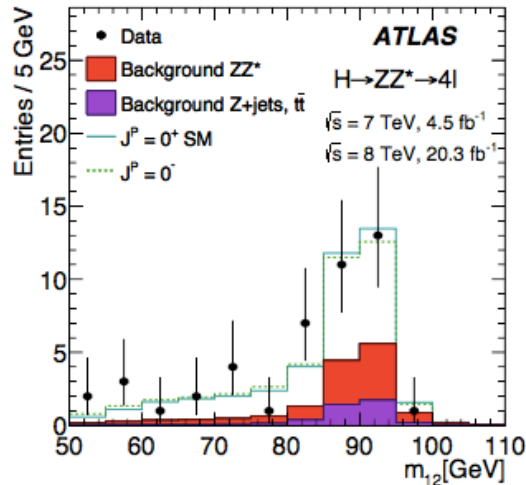


The choice of production and decay angles used in this analysis is presented in Figure 3, where the following definitions are used:

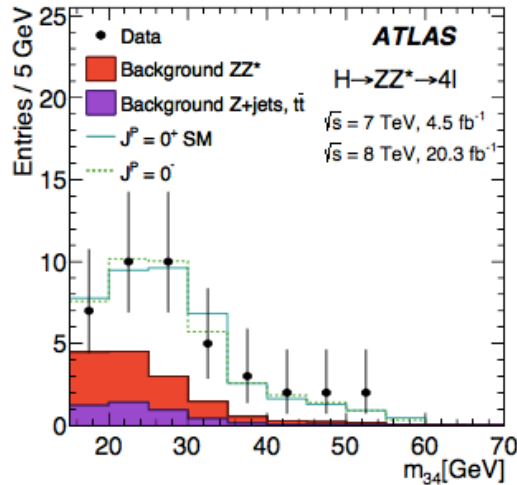
- θ_1 and θ_2 are defined as the angles between final-state leptons with negative charge and the direction of flight of their respective Z bosons, in the four-lepton rest frame;
- Φ is the angle between the decay planes of two lepton pairs (matched to the two Z boson decays) expressed in the four-lepton rest frame;
- Φ_1 is the angle between the decay plane of the leading lepton pair and a plane defined by the Z_1 momentum (the Z boson associated with the leading lepton pair) in the four-lepton rest frame and the positive direction of the collision axis;
- θ^* is the production angle of the Z_1 defined in the four-lepton rest frame.

Spin/parity from $H \rightarrow ZZ^* \rightarrow 4l$

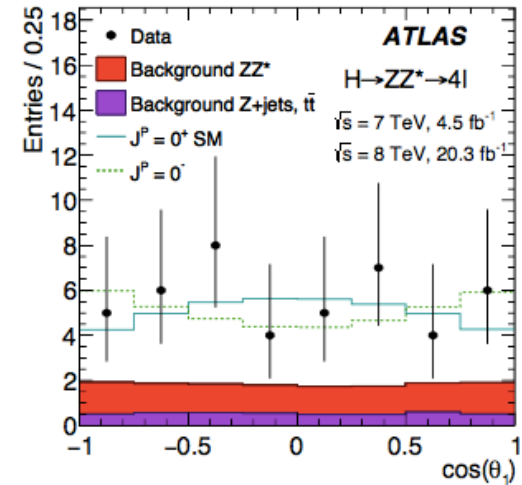
arXiv:1506.05669 (2015)



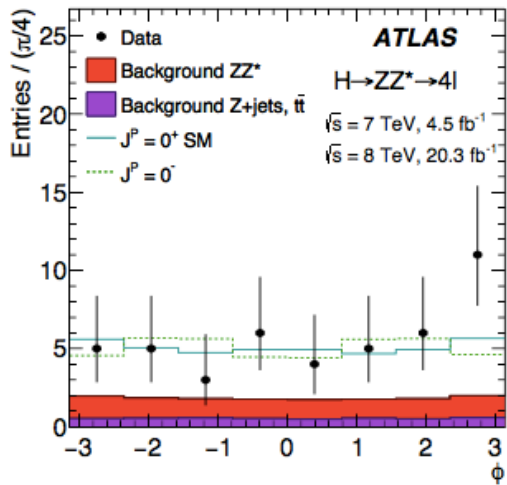
(a)



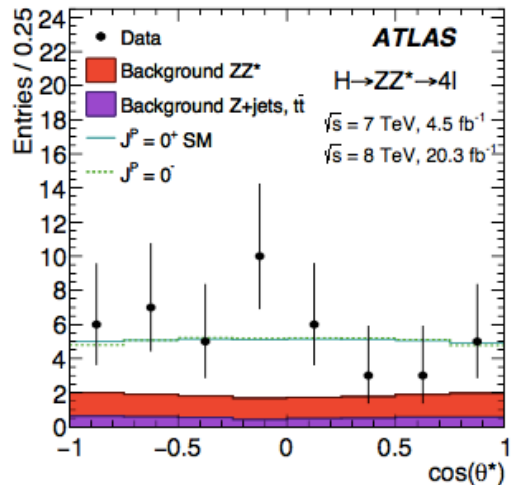
(b)



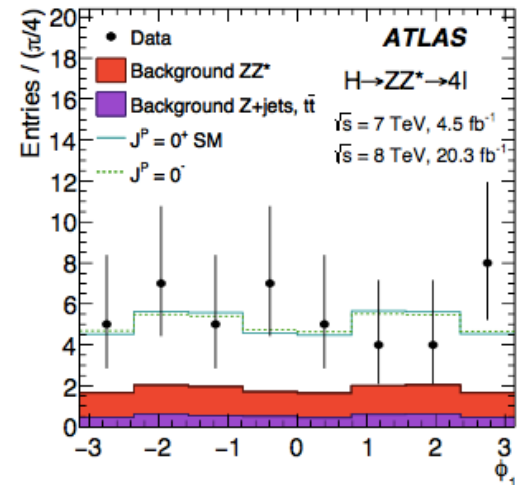
(c)



(d)



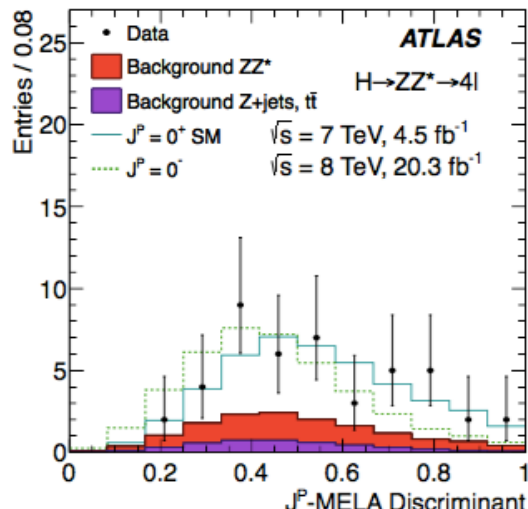
(e)



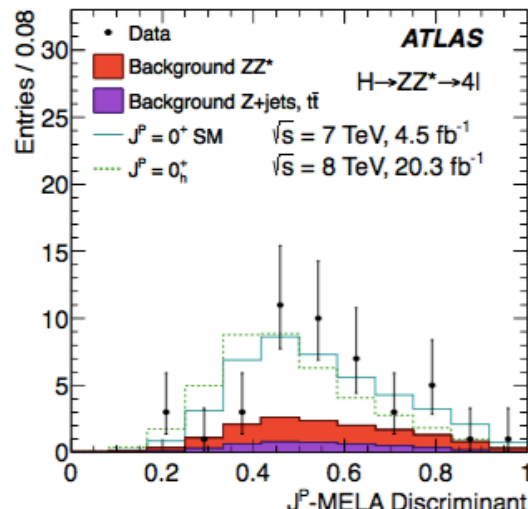
(f)

Spin/parity from $H \rightarrow ZZ^* \rightarrow 4l$

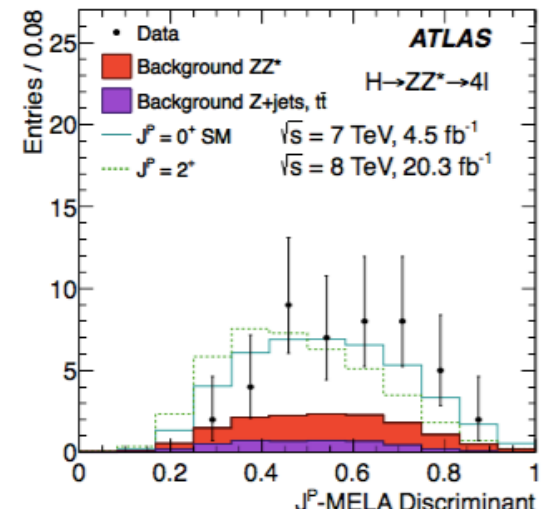
arXiv:1506.05669 (2015)



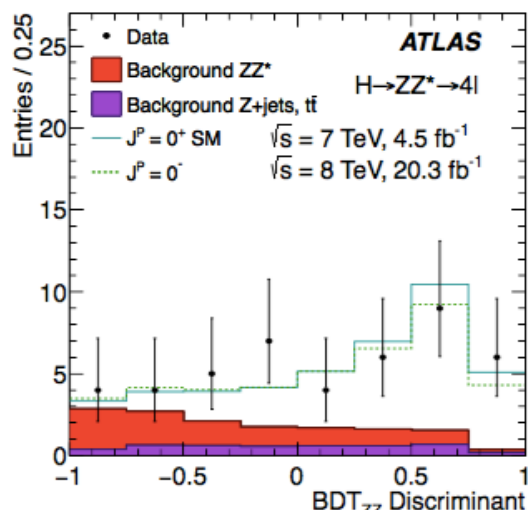
(a)



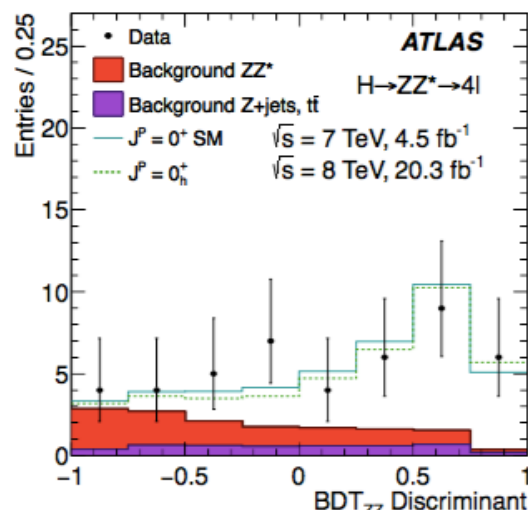
(b)



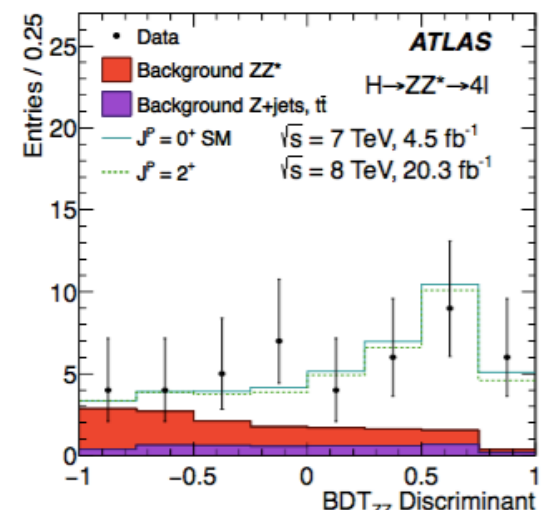
(c)



(d)



(e)



(f)

$H \rightarrow ZZ^* \rightarrow 4l$: MELA

[arXiv:1506.05669 \(2015\)](https://arxiv.org/abs/1506.05669)

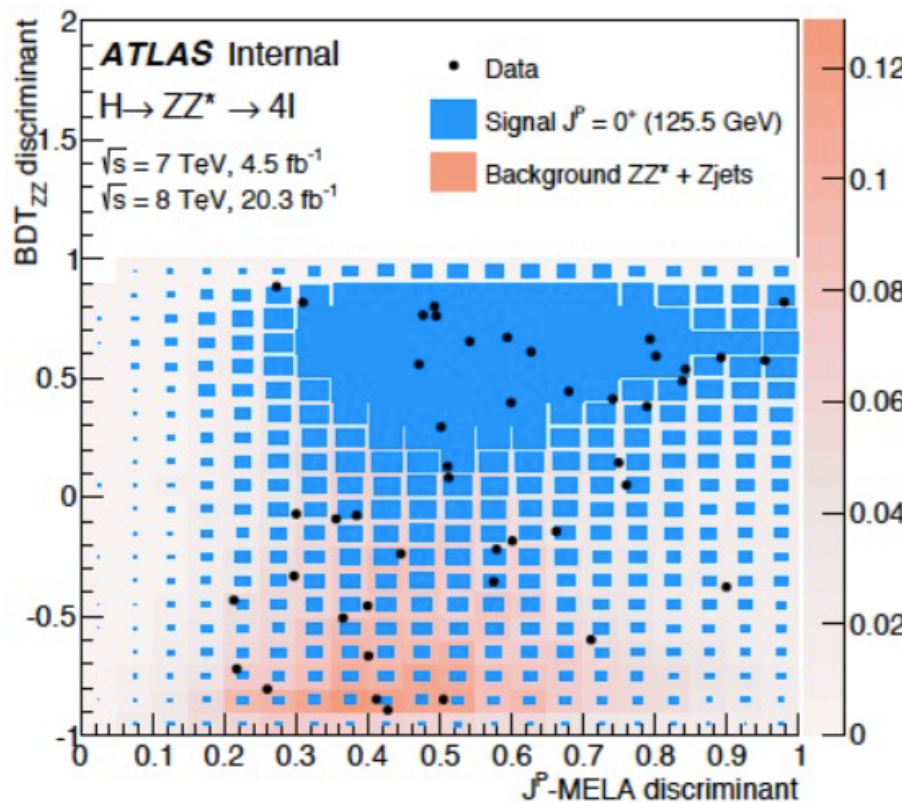


Figure 5: The distributions of the background discriminant BDT_{ZZ} versus the J^P – MELA discriminant for the $J^P = 0^+$ and $J^P = 0^-$ signal hypotheses in the signal region $115 \text{ GeV} < m_{4\ell} < 130 \text{ GeV}$.

Optimal Observables from Matrix Element

[arXiv:1506.05669 \(2015\)](https://arxiv.org/abs/1506.05669)

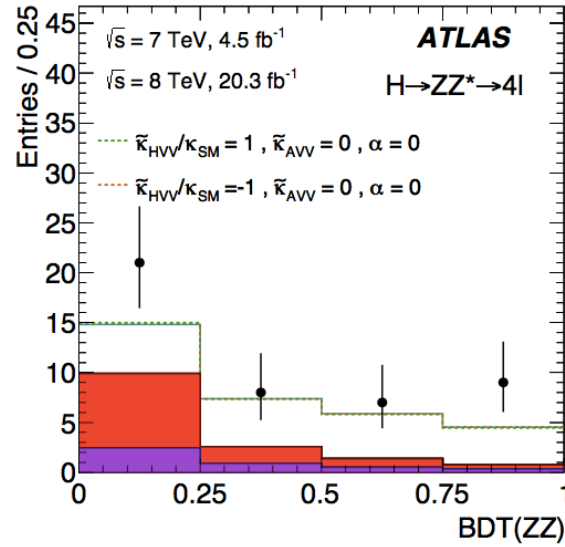
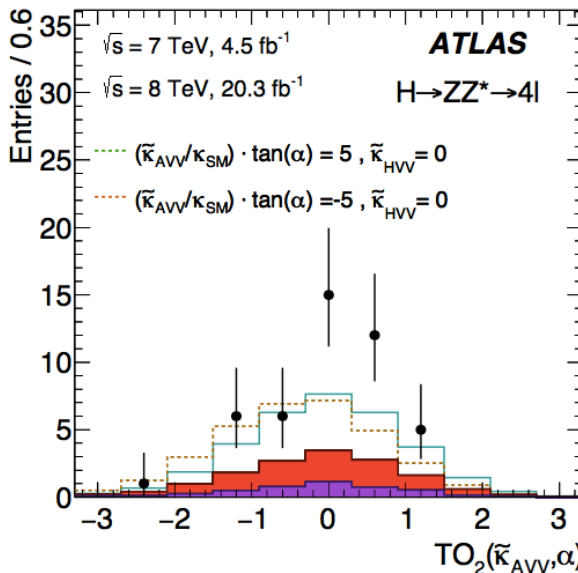
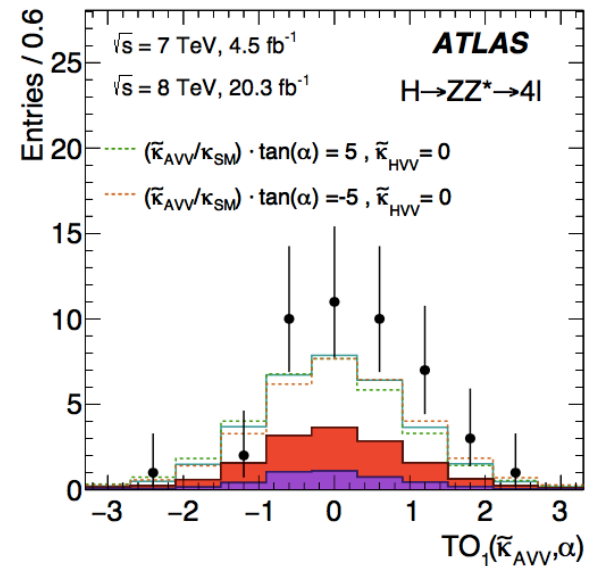
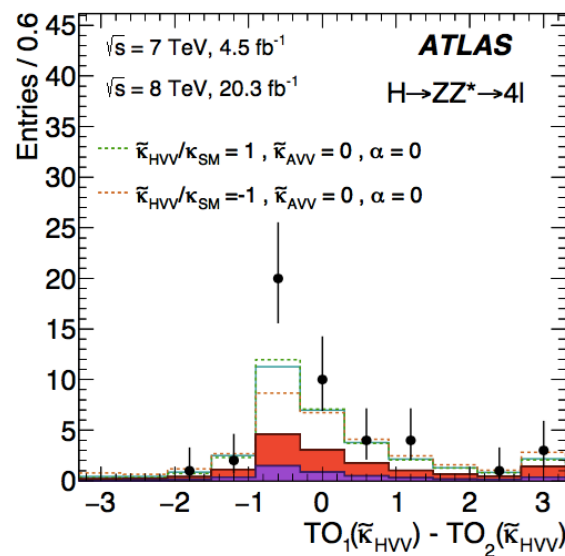
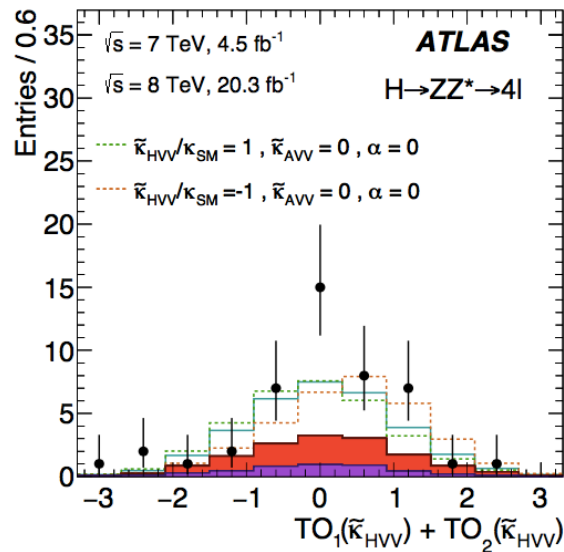
The observables sensitive to the presence and structure of κ_{SM} , κ_{HVV} and κ_{AVV} considered in the current analysis are defined as follows:

$$\begin{aligned} O_1(\kappa_{HVV}) &= \frac{2\Re[\text{ME}(\kappa_{SM}\neq 0; \kappa_{HVV}, \kappa_{AVV}=0; \alpha=0)^* \cdot \text{ME}(\kappa_{HVV}\neq 0; \kappa_{SM}, \kappa_{AVV}=0; \alpha=0)]}{|\text{ME}(\kappa_{SM}\neq 0; \kappa_{HVV}, \kappa_{AVV}=0; \alpha=0)|^2}, \\ O_2(\kappa_{HVV}) &= \frac{|\text{ME}(\kappa_{HVV}\neq 0; \kappa_{SM}, \kappa_{AVV}=0; \alpha=0)|^2}{|\text{ME}(\kappa_{SM}\neq 0; \kappa_{HVV}, \kappa_{AVV}=0; \alpha=0)|^2}, \\ O_1(\kappa_{AVV}, \alpha) &= \frac{2\Re[\text{ME}(\kappa_{SM}\neq 0; \kappa_{HVV}, \kappa_{AVV}=0; \alpha=0)^* \cdot \text{ME}(\kappa_{AVV}\neq 0; \kappa_{SM}, \kappa_{HVV}=0; \alpha=\pi/2)]}{|\text{ME}(\kappa_{SM}\neq 0; \kappa_{HVV}, \kappa_{AVV}=0; \alpha=0)|^2}, \\ O_2(\kappa_{AVV}, \alpha) &= \frac{|\text{ME}(\kappa_{AVV}\neq 0; \kappa_{SM}, \kappa_{HVV}=0; \alpha=\pi/2)|^2}{|\text{ME}(\kappa_{SM}\neq 0; \kappa_{HVV}, \kappa_{AVV}=0; \alpha=0)|^2}. \end{aligned} \tag{10}$$

Here $\text{ME}(\kappa_{SM}, \kappa_{HVV}, \kappa_{AVV}, \alpha)$ denotes the leading-order matrix element of the $H \rightarrow ZZ^* \rightarrow 4\ell$ process. These definitions correspond to the first- and second-order optimal observables for a BSM amplitude with a three-component structure.

To simplify their use in the analysis, all observables defined in Eq. (10) undergo a pdf transformation such that each observable becomes normally distributed in the Standard Model case. These transformed observables are referred to hereafter as $TO_{1,2}(\kappa_{HVV})$ and $TO_{1,2}(\kappa_{AVV}, \alpha)$ respectively.

Optimal Observables from Matrix Element

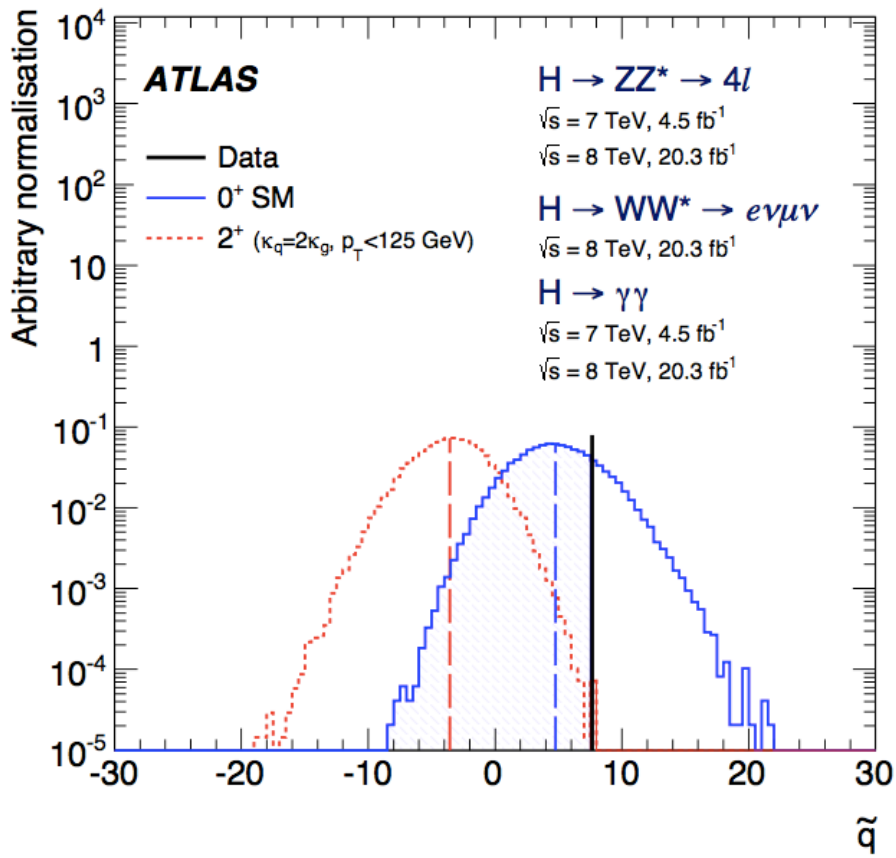
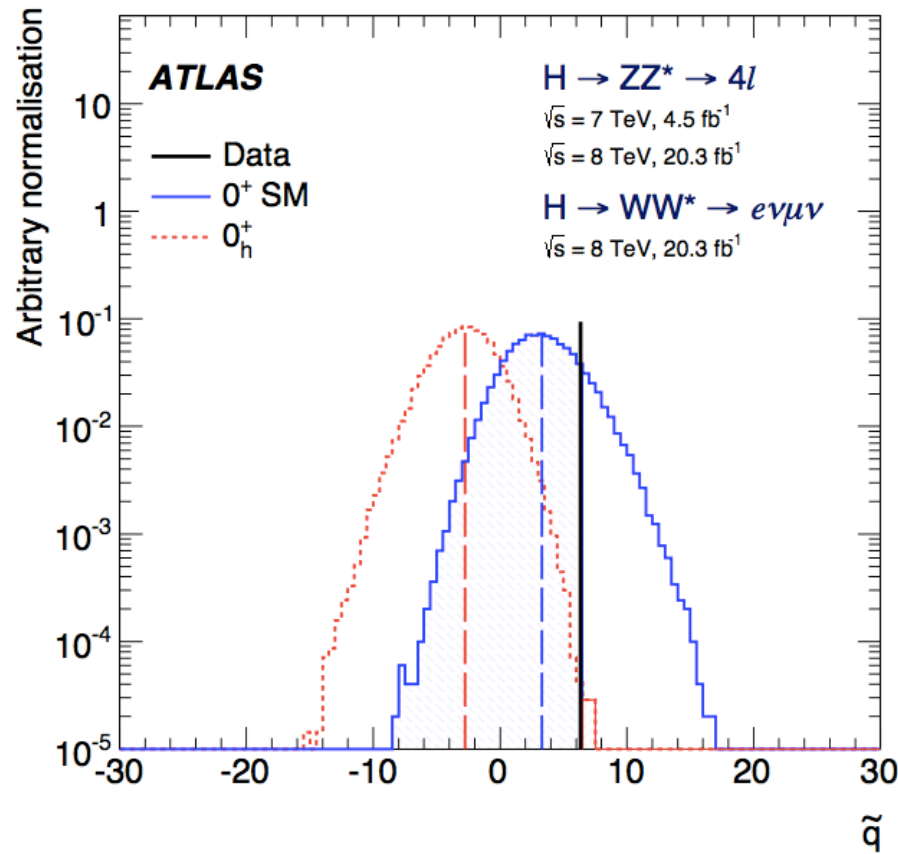


- Data
- Background ZZ^*
- Background $Z+jets, t\bar{t}$
- SM: $\kappa_{SM} = 1, \tilde{\kappa}_{HVV} = 0, \tilde{\kappa}_{AVV} = 0, \alpha = 0$

arXiv:1506.05669 (2015)

J^P hypothesis vs SM 0^+

[arXiv:1506.05669 \(2015\)](https://arxiv.org/abs/1506.05669)



Combined p-values

[arXiv:1506.05669 \(2015\)](https://arxiv.org/abs/1506.05669)

Tested Hypothesis	$p_{\text{exp}, \mu=1}^{\text{alt}}$	$p_{\text{exp}, \mu=\hat{\mu}}^{\text{alt}}$	$p_{\text{obs}}^{\text{SM}}$	$p_{\text{obs}}^{\text{alt}}$	Obs. CL _s (%)
0_h^+	$2.5 \cdot 10^{-2}$	$4.7 \cdot 10^{-3}$	0.85	$7.1 \cdot 10^{-5}$	$4.7 \cdot 10^{-2}$
0^-	$1.8 \cdot 10^{-3}$	$1.3 \cdot 10^{-4}$	0.88	$< 3.1 \cdot 10^{-5}$	$< 2.6 \cdot 10^{-2}$
$2^+(\kappa_q = \kappa_g)$	$4.3 \cdot 10^{-3}$	$2.9 \cdot 10^{-4}$	0.61	$4.3 \cdot 10^{-5}$	$1.1 \cdot 10^{-2}$
$2^+(\kappa_q = 0; p_T < 300 \text{ GeV})$	$< 3.1 \cdot 10^{-5}$	$< 3.1 \cdot 10^{-5}$	0.52	$< 3.1 \cdot 10^{-5}$	$< 6.5 \cdot 10^{-3}$
$2^+(\kappa_q = 0; p_T < 125 \text{ GeV})$	$3.4 \cdot 10^{-3}$	$3.9 \cdot 10^{-4}$	0.71	$4.3 \cdot 10^{-5}$	$1.5 \cdot 10^{-2}$
$2^+(\kappa_q = 2\kappa_g; p_T < 300 \text{ GeV})$	$< 3.1 \cdot 10^{-5}$	$< 3.1 \cdot 10^{-5}$	0.28	$< 3.1 \cdot 10^{-5}$	$< 4.3 \cdot 10^{-3}$
$2^+(\kappa_q = 2\kappa_g; p_T < 125 \text{ GeV})$	$7.8 \cdot 10^{-3}$	$1.2 \cdot 10^{-3}$	0.80	$7.3 \cdot 10^{-5}$	$3.7 \cdot 10^{-2}$

Combined Tensor Coupling Ratio

arXiv:1506.05669 (2015)

